

SIMULATION OF A HUMAN THERMOREGULATORY SYSTEM
WITH DRY ICE COOLING

by

BALDEV SINGH DHIMAN

B.S. (Engg), Punjab University, 1969

A MASTER'S THESIS

submitted in partial fulfilment of the
requirements for the degree

MASTER OF SCIENCE

in

INDUSTRIAL ENGINEERING

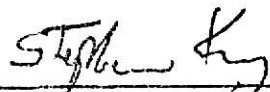
Department of Industrial Engineering

KANSAS STATE UNIVERSITY

Manhattan, Kansas

1974

Approved by:


Major Professor

**THIS BOOK
CONTAINS
NUMEROUS PAGES
WITH THE ORIGINAL
PRINTING BEING
SKEWED
DIFFERENTLY FROM
THE TOP OF THE
PAGE TO THE
BOTTOM.**

**THIS IS AS RECEIVED
FROM THE
CUSTOMER.**

LD
2668
T4
1974
D48
C.2
Document

11

TABLE OF CONTENTS

	Page
ACKNOWLEDGEMENTS	
LIST OF TABLES	
LIST OF FIGURES	
INTRODUCTION	1
LITERATURE REVIEW	2
PROBLEM	
Controllers	6
Artificial controllers	7
PROPOSAL	
Objectives	9
Modes of heat transfer	11
Subject	13
Model outline	14
The controlled system	16
Stolwijk's controlling system	31
Measurements and procedure	39
RESULTS	
Nude man	43
Dry ice vest	54
DISCUSSION	67
SUMMARY AND CONCLUSIONS	71
REFERENCES	72
APPENDIX	76

ACKNOWLEDGEMENTS

The author is grateful to his major professor Dr. Stephan Konz for providing both personal encouragement and technical guidance during all phases of this work. Dr. C. L. Hwang deserves special thanks for his guidance in the area of mathematical modeling.

Thanks go to Abu Masud for help during latter part of the work.

LIST OF TABLES

	page
1. Experimental conditions.	10
2. List of symbols used in the controlled system with definition and dimensions.	17
3. Distribution of surface area and volume over the six segments.	19
4. Distribution, by weight, of different tissue types over the six segments, in % of total.	21
5. $C(N)$, heat capacitance of compartment N, kcal/C/gm.	22
6. $QB(N)$, basal metabolic rate in compartment N, kcal/h.	24
7. $EB(N)$, basal evaporative heat loss in compartment N, kcal/h.	25
8. $BFB(N)$, basal blood flow in compartment N, litres/h.	27
9. Estimation of thermal conductance between layers.	28
10. Calculated combined environmental heat transfer coefficient for a nude man, standing in a room where wall and air temperature are the same.	30
11. Definition of symbols used in the description of the controlling system.	32
12. Tentative estimates of distribution of sensory input, effector output over the skin, and of heat production in muscle during work and shivering.	40
13. $TSET(N)$, set point temperature for receptors in N, deg C	68
14. Initial input temperatures, deg C	69

LIST OF FIGURES

	page
1. Stolwijk's original representation of the human trunk.	12
2. Simplified block diagram of human thermoregulation.	15
3. Block diagram of the controlled system for one segment: the head.	18
4. Rectal temperature (nude man).	45
5. Head skin temperature (nude man).	46
6. Trunk skin temperature (nude man).	48
7. Arm skin temperature (nude man).	49
8. Average of calf and thigh temperature (nude man).	51
9. Cardiac output and $HR \cdot SBP$ (nude man).	53
10. EVAPR and EV (nude man).	55
11. Rectal temperature (dry ice vest).	58
12. Head skin temperature (dry ice vest).	59
13. Trunk skin temperature (dry ice vest).	60
14. Trunk skin temperature (dry ice vest).	61
15. Arm skin temperature (dry ice vest).	63
16. Average of calf and thigh temperature (dry ice vest).	64
17. Cardiac output and $HR \cdot SBP$ (dry ice vest).	65
18. EVAPR and EV(dry ice vest).	66

INTRODUCTION

The dynamics of temperature regulation in man have been of interest to physiologists for years. This interest has manifested itself in over 4000 papers (6) published on the subject of thermoregulation during the last thirty years or so. However, as we progress in the study of body temperature regulation, it is evident that the complexity of the system is such that it becomes increasingly difficult to rely on an intuitive approach to the design of optimal experiments or to the interpretation of experimental data. This is probably an important reason why it is useful to formulate quantitative models of the thermoregulatory control system. Models of this nature have been proposed by Wyndham et al (51), Wissler (49), Smith and James (37), Stolwijk and Hardy (42), Crosbie et al (15), and others.

Development of a mathematical model of the thermoregulation system is an educating experience. Important contributions of mathematical models are in the areas of evaluation and interpretation of experimental results. Models may also suggest the way for suitable experiments to challenge expressed concepts. If a proposed mechanism of thermoregulation is expressed in quantitative form, it describes the relationship between the input signals and the resulting thermoregulatory response. The model can be used to compare the quantitative response resulting from a proposed mechanism with the response obtained by measurements. It is understood that such models are to be used in close connection with an experimental program. An excellent review on mathematical models of human thermoregulation has been given by Fan et al (18).

LITERATURE REVIEW

Early work on the nature of thermoregulation can be traced to Liebermeister (30). As far back as 1871, he discussed fevers in terms of imbalance of heat production and heat loss controlled by centers in the brain. Later, Richet (35) and Ott (32) furnished experimental evidence about the role of the hypothalamus in the control of body temperature. Barbour (3) demonstrated in 1929 that the hypothalamus functioned much like a thermostat. Work of Bazett and Penfield (4), Keller and Hare (25), Hemingway (23), Thauer (44) and others have identified more clearly the function of the nervous system in thermoregulation. The role of the anterior hypothalamus in physiological control of mammalian body temperature was first clearly demonstrated by Magoun, Harrison, Brobeck, and Ranson (30).

With the passage of time, a greater amount of information became available regarding heat transfer within the body and the nature of heat exchange between the body at its skin surface and the environment. Several attempts were made to treat thermoregulation as a system. Burton (11), Hardy (20), and Wyndham et al (51) made attempts in this direction. This stimulated further experimental work directed at achieving a better understanding of the various elements of the system and the operation of the system as a whole (Hardy and Hammel (21), Crosbie et al (15)). In most instances, conceptual models of thermoregulation were elaborated to account for specific experimental findings (Benzinger (5), Hammel et al (19)). Many attempts were also made to construct analytical models from available data. Considerable literature

has been published about analytical models. Some of the models have been established on the basis of experiments. Others have been formulated on the theories of thermodynamics and transport processes. These analytical models were used to predict physiological results by simulating thermal disturbances so that comparisons between theory and experiment were possible. Wyndham and Atkins (51), Hardy (20), Wissler (48), Smith and James (37) and others constructed models of physiological temperature regulation.

Wyndham and Atkins (51) approximated the body by a series of concentric cylinders corresponding to the core, muscle, and skin. In their analysis, they only considered the radial heat flow. By using a numerical technique and an analog computer, they obtained transient solutions for their model.

Crosbie et al (15) employed a similar technique and applied it to a one-dimensional slab model. They assumed the slab to be divided into three layers corresponding to the core, muscle, and skin. Each of the layers was assigned constant, uniform, but different temperatures. The simulation results were compared with physiological data. Neither of the latter two approaches explicitly included a blood flow term.

In 1961 Wissler (46) initiated his study of modeling of the human thermal system. He divided the body into six cylinders corresponding to the arms, legs, trunk, and head. Including a blood flow term, he obtained analytical solutions for radial heat transfer for both the steady and transient states. He also introduced the concept of a central "pool", where blood from all regions is gathered, mixed, and

redistributed, and the idea of the lumped heat exchange between arteries and veins. In 1964 he improved his model by dividing the body into fifteen circular cylinders interconnected by blood vessels (48). Hsu, in 1971 (24) presented a model of human thermoregulation based upon one of Wissler's models.

Perl, in 1962 (33), advanced the idea of indirect measurement of blood flow rates by employing Fick's second principle. He solved analytically the steady state and the transient problems and compared his results with experiments.

An analog computer was employed by Brown in 1963 (9) for simulating temperature regulation in man. He divided the body into four regions (central, muscle, subcutaneous region, and skin). He studied heat distribution within the body and also the interaction between the body and the environment. Numerical solutions for a unidimensional, four layer transient model were also obtained by Layne and Barker (28) in 1965 and by Stolwijk and Cunningham (40).

In 1966 Stolwijk and Hardy (42) represented the human body by three cylinders corresponding to the head, trunk, and extremities. The ends were assumed to be perfectly insulated. Each of the cylinders was subdivided into two or more concentric layers to represent the skin, muscle, viscera, brain etc., and each sublayer was assumed to be at a constant temperature. Only radial heat flow was assumed. The effect of blood flow, as well as metabolic heat production, was included. Eight simultaneous differential equations were written for the various sublayers and three "controller" equations. The three controller equations

corresponded to evaporative heat losses, muscle blood flow changes with temperature and exercise rate. The effects of shivering on heat transfer were also included. The set of equations was solved on an analog computer. Transient temperature distributions for various environmental and metabolic conditions were obtained. Stolwijk and Hardy were the first to introduce the concept of the passive system and an active controller as applied to the human thermoregulatory system. According to this concept, the passive system represents a complex transfer function between the controller and the disturbance. The controller is responsible for maintaining the human body within the narrow limits of acceptable thermal conditions by activating the four thermoregulatory mechanisms, i.e., vasoconstriction, vasodilation, sweating, and shivering.

PROBLEM

Controllers. When man is exposed to a heat stress environment, the body thermoregulatory system adjusts the various regulatory functions to maintain a state of thermal neutrality. The body has four active controllers for maintaining itself in an essentially isothermal state. The active controllers are:

- (1) Sweating
- (2) Shivering
- (3) Vasodilation
- (4) Vasoconstriction

Man's best protection against heat is his ability to use the evaporative cooling resulting from his sweating. Sweating is caused by temperature stimuli from both the skin and core. There are both local controls and central controls. Sweating is not an uncomfortable process as long as moisture can evaporate freely from the skin surface. Discomfort occurs when the same rate of sweating requires a larger wetted surface on the skin from which it must evaporate. Sweating at very high levels is generally accompanied by active vasodilation. Excessive sweating can cause swelling of the extremities, skin irritation, headaches and throbbing due to increased heart action.

The purpose of active shivering is analogous to, but has the opposite effect of, sweating. Heat is generated by shivering. The body shivers to increase the metabolic rate in order to compensate for excessive heat loss. Shivering can only occur in cold environments.

Vascular control of blood flow to and from the skin surface is a method by which the body can change the flow of heat from its central core to the environment. Vasodilation always occurs during regulatory sweating. Vasoconstriction is usually associated with a cold stress.

The equations describing the active human thermoregulatory control are highly empirical. The state of the art is such that these equations and coefficients are especially subject to change.

Artificial controllers. The active controllers described above are not sufficient for body thermoregulation in excessively severe hot environments (over 40 deg C) and over prolonged exposures. This means that man's natural physiological abilities have to be augmented to cope with increased heat stress. The required artificial systems provide micro-climates to man that are capable of reducing environmental heat stresses. The two most widely used methods for providing micro-climates are:

- (1) gas-ventilated garments,
- (2) liquid cooled garments.

Conceptually the two processes are drastically different. The gas-ventilated garment is designed to provide a gas flow (e.g. air or oxygen). This gas flow over the body provides both sensible cooling (heating of the gas stream) and latent cooling (evaporation of sweat). If the gas temperature is less than the body's, the heat load is reduced by convection also. In the liquid cooled garment, cooling is provided by conduction. A network of cooling tubes is held in contact against the body surface.

An interesting alternative system for providing a micro-climate to man is currently under investigation at Kansas State University by Konz et al (27). This system utilizes a dry ice garment to provide the cooling effect. Model A of the dry ice garment was used in the experiments by Konz et al (27). The garment consists of pockets sewed to a net, stitched in the shape of a vest. The outside of a pocket is felt-like. Inside there are two layers of insulation-- an inner one of plastic foam and an outer one of plastic film with entrapped air bubbles. Dry ice slabs are put in the pockets of the vest which is then worn over the bare skin. The dry ice garment provides cooling by conduction. The garment picks up heat from the body (some heat is also drawn from the environment) and the dry ice sublimates in the process. The sublimation of dry ice provides a cooling capacity of 160 kcal/kg as shown below if skin temperature is assumed to be 35 C:

Sublimation	137 kcal/kg
Gas temperature rise $.208 \times (35 - (-79))$	<u>23 kcal/kg</u>
Total	160 kcal/kg

Initially the dry ice cooling investigation was carried out by using a Japanese garment of six pocket design. Later the garment was modified to have twelve pockets-- Model A. An improved version, Model B, is under development, but this paper will use data only from Model A.

This control of the body's microthermal environment may be called substitutive thermoregulation as the objective is to suppress natural thermoregulatory mechanisms. No attempt was made to present a detailed

comparative analysis of the three systems described above (gas cooling, liquid cooling, and dry ice cooling). However, a dry ice cooling system offers advantages in the following areas:

- (1) Low initial cost of the dry ice cooling garment (below \$50.00 for models presently available).
- (2) Low operating cost. Dry ice is available @ 35¢ per kg in most areas. The twelve-pocket garment uses about 5 kgs of dry ice per 8 hours. Cost per hour is 25¢.
- (3) Lack of moving parts.
- (4) No tether such as in liquid cooled garments.

Thus, considering all its advantages, dry ice cooling is an interesting potential system for further investigation.

Objective. The objective of this study was to develop a revised mathematical model of the human thermoregulatory system with dry ice cooling. Specifically, it was proposed to model the dynamic response of the human thermal system exposed to a heat stress environment (43.3 C, RH = 45%). The mathematical model was validated using experimental data already obtained by Konz et al (27) in their experiments in the summer of 1972. This data is shown in Table 1.

The mathematical model described by Stolwijk (38) formed the basis of this study. This model divides the human body into six segments: 1) head, 2) trunk, 3) arms, 4) hands, 5) legs, 6) feet. Each segment is further subdivided into four layers: 1) core, 2) muscle, 3) fat, 4) skin. In addition, a central blood compartment links the six segments together via appropriate blood flow to each of the segments. This makes

Table 1

Experimental Conditions

In all experiments the dry bulb temperature was 43.3°C, the mean radiant temperature was 42.8°C and the subject sat reading.

Initial Gr	Dry Ice		No. of Pockets	Outer Jacket	Extra Insulation	Air Velocity, m/s	Relative Humidity, %	Date
	SA Facing mm ²	SA Total mm ²						
0	0	0	6	No	No	.1	45	7/5
0	0	0	12	No	No	.1	45	7/31
0	0	0	12	No	No	.1	55	7/24
849	37,000	115,000	6	No	No	.1	45	6/23
871	37,000	115,000	6	No	No	.1	45	6/26
870	37,000	115,000	6	No	Yes	.1	45	7/10
887	37,000	115,000	6	No	Yes	.1	45	7/7
908	37,000	115,000	6	No	No	.4	45	7/14
1007	37,000	115,000	6	No	Yes	.1	45	7/12
907	42,000	121,000	12	No	No	.4	55	7/17
2187	62,000	204,000	12	Yes	No	.1	55	7/21
2251	89,000	159,000	12	Yes	Yes	.1	45	8/7
2663	76,000	244,000	12	Yes	Yes	.4	45	8/2
2762	75,000	240,000	12	Yes	Yes	.1	45	8/1
2868	77,000	250,000	12	No	No	.1	45	7/28
2870	79,000	251,000	12	Yes	No	.1	45	7/26
3159	89,000	273,000	12	Yes	Yes	.1	45	8/8
3309	89,000	275,000	12	No	No	.1	55	7/19

a total of twenty-five compartments into which the whole human body was divided. Fig. 1 shows a schematic of the human trunk based upon Stolwijk's original data (38).

The study involved:

- A: Development of a revised mathematical model of the human thermoregulatory system. It consisted of 1) revised model. 2) Determination of the overall heat transfer coefficient. 3) Computer program necessary to carry out simulations.
- B: The revised mathematical model was used to simulate the response of the human thermoregulatory system for a man exposed to a hot environment.
- C: Validation/updating of the revised model.

Modes of heat transfer

It is necessary at this stage to consider the mode of heat transfer between the human thermal system and its environment. The heat exchange between the human thermal system and the environment takes place at the skin surface. Heat is produced by the oxidation of fuel for energy and heat is dissipated by conduction, convection, radiation, and mass transfer at the skin surface. Heat produced in excess of that which can be dissipated will be stored in the tissues with a resulting rise in body temperatures. Heat storage in excess of 100 kcal (a rise in body temperature of about 1.2 °C.) represents the onset of physiological stress. Heat generated in the body compartments is transmitted by convection to blood, and by conduction to adjacent compartments. From

**THIS BOOK
CONTAINS
NUMEROUS PAGES
WITH DIAGRAMS
THAT ARE CROOKED
COMPARED TO THE
REST OF THE
INFORMATION ON
THE PAGE.**

**THIS IS AS
RECEIVED FROM
CUSTOMER.**

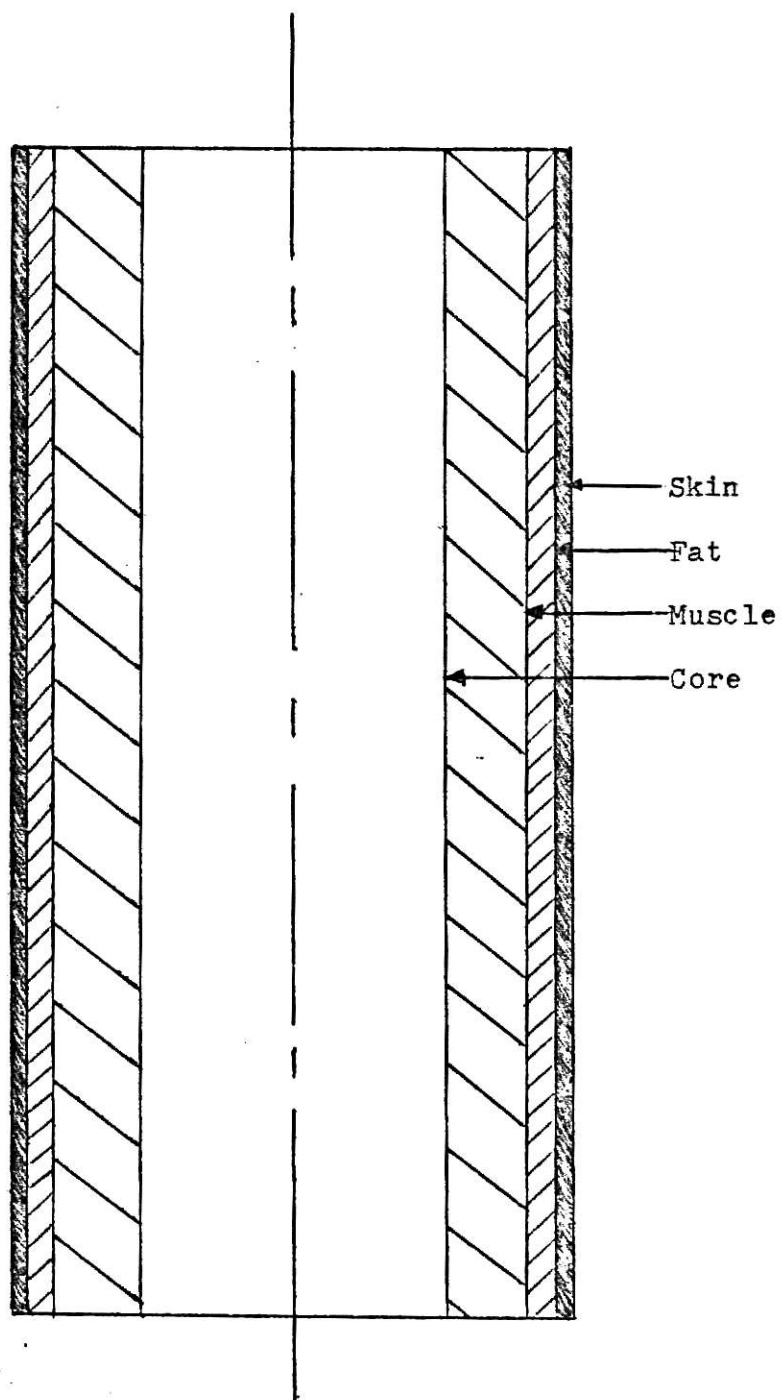


Figure 1. Stolwijk's original representation of the human trunk.

the skin, the heat transfer is by: 1) convection to the air, 2) radiation to walls or to the garment interior surfaces, 3) evaporation and 4) conduction to the cooling garment.

The equation for the body heat balance can be written as follows:

$$M + S = -E + R + C + K - W$$

Where M - Metabolic production, kcal/h
 E - Evaporative heat loss, kcal/h
 R - Radiant heat exchange, kcal/h
 C - Convective heat exchange, kcal/h
 K - Conductive heat exchange, kcal/h
 W - Work, kcal/h
 S - Rate of storage of body heat, kcal/h
 ($S = 0.0$ at equilibrium)

Subject. In the simulation model the data gathered by Konz et al (27) was used to compare predicted results with actual responses obtained during experiments. These experiments were carried out at Kansas State University on a subject whose mean body weight was 77 kg and height was 177 cms. His mean calculated surface area using DuBois' formula was 1.9 m^2 .

It was necessary to convert the various control coefficients used by Stolwijk to fit our subject as the weight and body dimensions of Stolwijk's subject differed from our subject. (Stolwijk used the DuBois' formula to calculate a surface area of 1.89 m^2 for his 74.1 kg man).

Model outline

Fig. 2 represents a simple division of the thermoregulatory system. The figure shows a controlling system and a controlled system.

The controlled system is the biothermal mass of the body. In the controlled system, the body is divided into six segments. Each segment is further subdivided into four layers. The six segments are linked together by the central blood compartment via the appropriate blood flows to each of the segments. Thus we have a total of twenty-five compartments. Twenty-five basic heat balance equations-- one for each compartment-- form the core of the model.

The temperature in each of the twenty-five compartments is an input into the controlling system. The resulting effector output from the controlling system can be applied to any part of the controlled system. In addition, all the appropriate parts of the controlled system can interact with the environment.

The controlling system receives from all layers in each segment 1) the instantaneous temperature, and 2) the rate of change of temperature. Thus there can be any number of combinations of receptor outputs. Any combination of receptor outputs so derived can be integrated in a number of different ways, and translated into effector command signals. These signals are distributed to the appropriate layers in each segment, where they may be subject to local modulation. The resulting effector actions are applied to the controlled system.

Yamamoto and Raub (52), in their proposed models of the respiratory control system, have presented symbol tables and equations in a Fortran

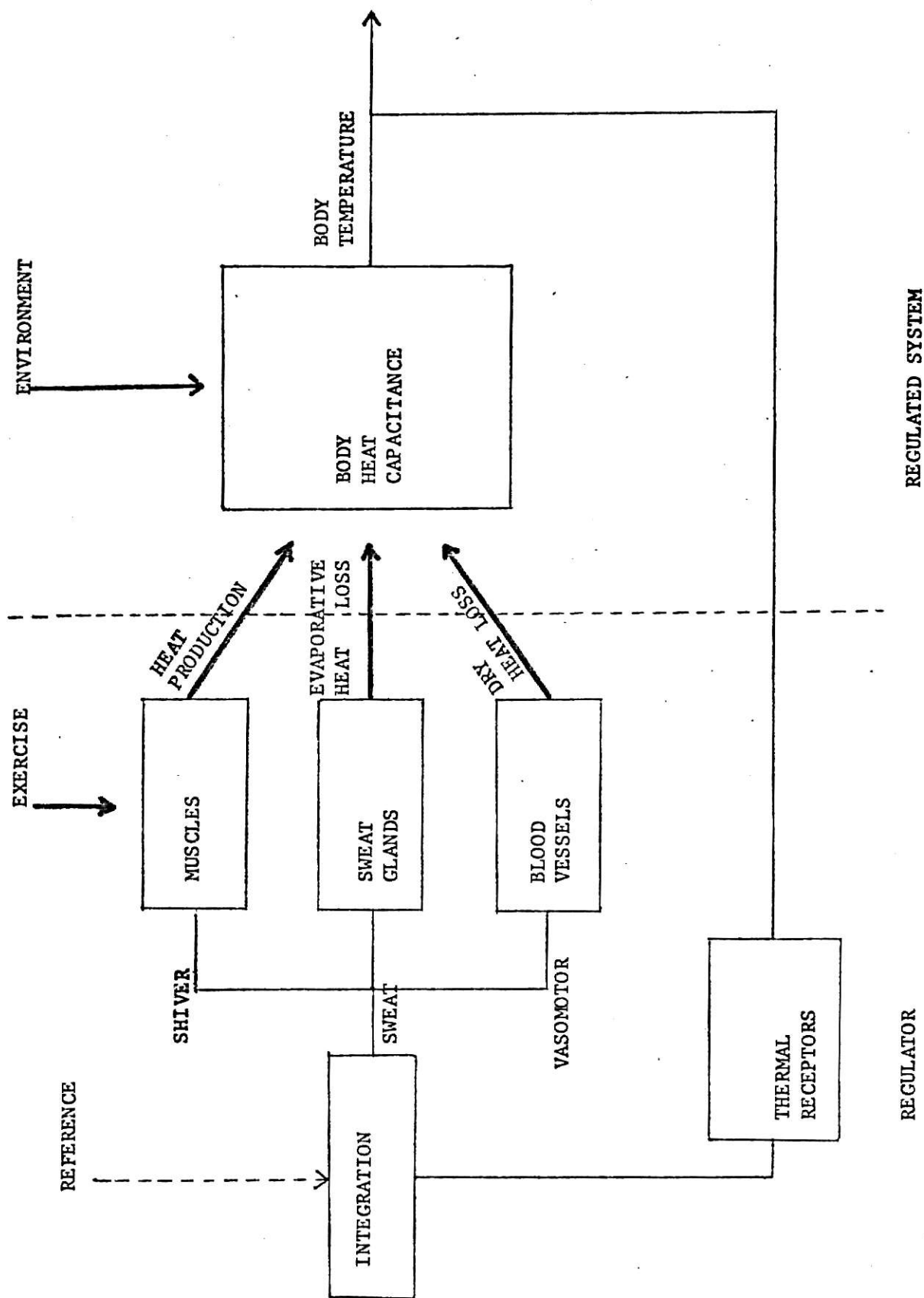


Figure 2. Simplified block diagram of human thermoregulation (38).

notation. The same convention was also followed in this work. It is hoped that the symbols will be found acceptable for use by others. A complete list of the symbols used in the controlled system, with their definitions and dimension, is given in Table 2.

The controlled system

Fig. 3 represents a schematic diagram for one segment of the controlled system, in this case the head. Each compartment represents a lumped heat capacitance with its own metabolic heat production. Each compartment exchanges heat by conduction to adjacent layers, and by convection via the blood. Associated with each compartment is an evaporative heat loss.

Meeh (31), DuBois and DuBois (16), and Bradfield (7) carried out measurements for surface area on ten men and ten women each. Their works formed the basis for the surface area and volumes values shown in Table 3. Volume measurements by Stolwijk (38) were carried out on five men and five women by measuring the circumferences and lengths of the various segments. The volumes of the hands and feet were measured by displacement.

Using the data in Table 3 and the equation proposed by DuBois and DuBois (17), Stolwijk estimated the surface area and weight of each segment. The DuBois equation for surface area is;

$$S = .007184 W^{.425} H^{.725}$$

in which S = surface area in m^2 ,

W = weight in kg,

H = height in cms.

TABLE 2

LIST OF SYMBOLS USED IN THE CONTROLLED SYSTEM WITH DEFINITION AND DIMENSIONS

Symbol	Vector Length	Definition	Dimensions
C(N)	25	Heat capacitance of compartment N	kcal · °C ⁻¹
T(N)	25	Temperature of N	°C
F(N)	25	Rate of change of temperature in N	°C · h ⁻¹
HF(N)	25	Rate of heat flow into or from N	kcal · h ⁻¹
TC(N)	24	Thermal conductance between N and N + 1	kcal · h ⁻¹ · °C ⁻¹
TD(N)	24	Conductive heat transfer between N and N + 1	kcal · h ⁻¹
QB(N)	24	Basal metabolic heat production in N	kcal · h ⁻¹
Q(N)	24	Total metabolic heat production in N	kcal · h ⁻¹
EB(N)	24	Basal evaporative heat loss from N	kcal · h ⁻¹
E(N)	24	Total evaporative heat loss from N	kcal · h ⁻¹
BFB(N)	24	Basal effective blood flow to N	l · h ⁻¹
BF(N)	24	Total effective blood flow to N	l · h ⁻¹
BC(N)	24	Convective heat transfer between central blood and N	kcal · h ⁻¹
HC(I)	6	Convective and conductive heat transfer coefficient for Segment I	kcal · m ⁻² · h ⁻¹ · °C ⁻¹
S(I)	6	Surface area of Segment I	m ²
HR(I)	6	Radiant heat transfer coeff. for Segment I	kcal · m ⁻² · h ⁻¹ · °C ⁻¹
H(I)	6	Total environmental heat transfer coeff. for Segment I	kcal · h ⁻¹ · °C ⁻¹
V		Air velocity	m · sec ⁻¹
TAIR		Effective environmental temperature	°C
RH		Relative humidity in environment	—
TIME		Elapsed time	h
PAIR		Vapor pressure in environment	mm Hg
ITIME		Elapsed time	min
INT		Interval between outputs	min
DT		Integration step	h
P(I)	10	Vapor pressure table from 5-50°C	mm Hg
EMAX (I)	6	Cal. max. rate of evaporative heat loss from Segment I	kcal · h ⁻¹
WORK		Total metabolic rate required by exercise	kcal · h ⁻¹
PSKIN		Saturated water vapor pressure at skin temperature	mm Hg

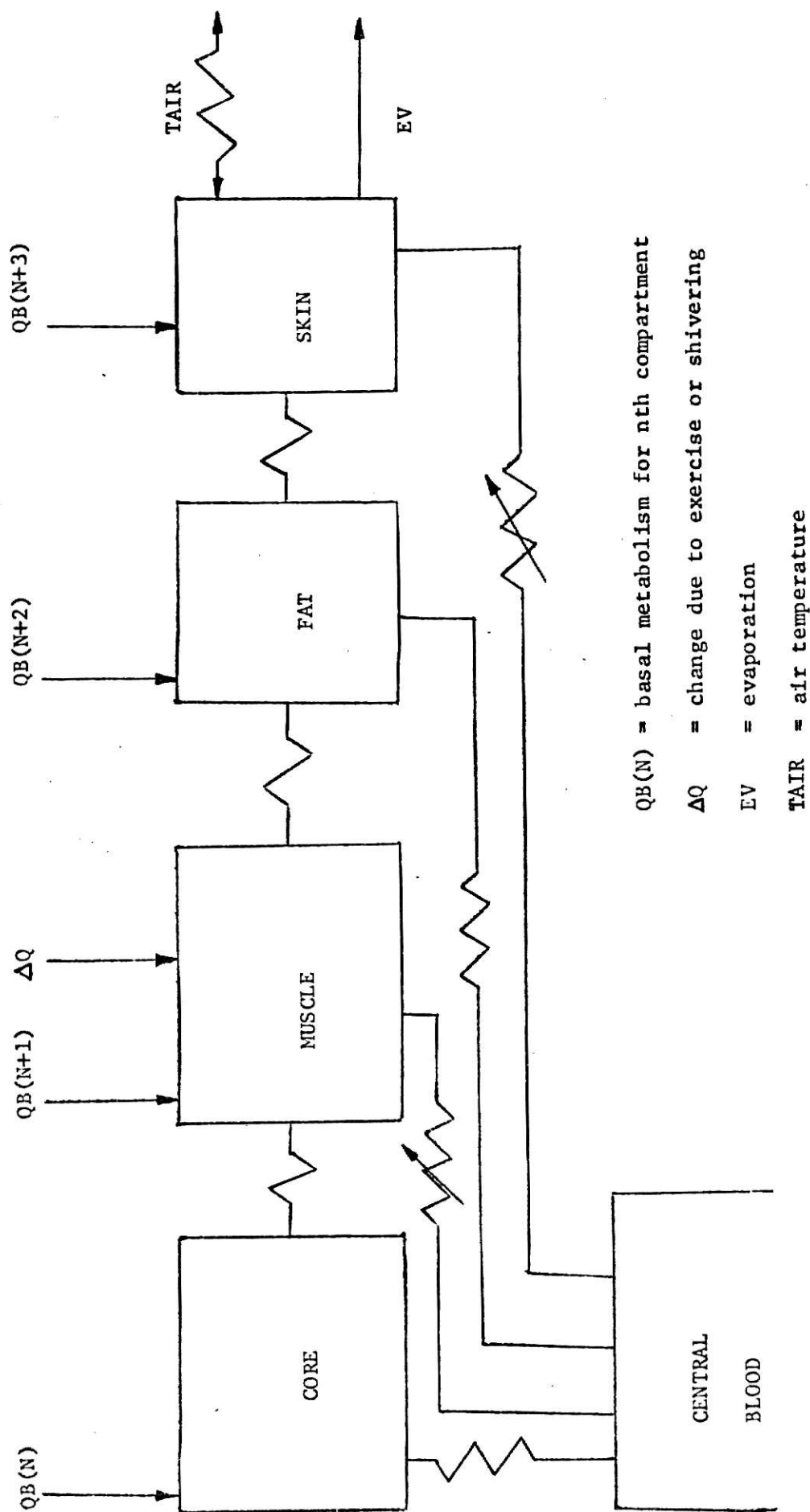


Figure 3. Block diagram of the controlled system for one segment : the head (38).

TABLE 3

DISTRIBUTION OF SURFACE AREA AND VOLUME OVER THE SIX SEGMENTS

Segment	Surface Area m ²		Surface Area %		Volume %		Average, % of Total	
	10 Men	10 Women	Men	Women	Men	Women	Surface Area	Volume
Head	0.1326	0.1129	7.00	6.49	5.34	5.58	6.74	5.46
Trunk	0.6804	0.6279	36.02	36.07	56.70	57.00	36.05	56.85
Arms	0.2536	0.2210	13.41	12.70	7.78	6.52	13.05	7.15
Hands	0.0946	0.0783	5.00	4.50	0.88	0.90	4.75	0.89
Legs	0.5966	0.5904	31.74	33.92	27.90	28.70	32.83	28.30
Feet	0.1299	0.1100	6.86	6.32	1.43	1.34	5.59	1.38
Total	1.8877	1.7404	100.0	100.0	100.0	100.0	100.0	100.0

The DuBois surface area for our subject worked out to 1.9 m^2 . However, van Graan (45) has reported that the DuBois formula underestimates the surface area of the body. Using the modification proposed by him, we obtained a new surface area for our subject of 2.0367 m^2 .

Wilmer (46) has given the distribution of tissue in the adult human body as:

<u>Tissue</u>	<u>%</u>
Skin and fat	25
Viscera	11
Nervous tissue	3
Muscle	43
Skeleton	$\frac{18}{100}$

Scammon (36) gives the average weights of different body parts and structures. This formed the basis for the values given in Table 4.

For calculating the heat capacitances (C(N)), given in Table 5, assumptions about the specific heats of various tissue types were made as follows:

- 1) Fat tissue - $0.6 \text{ gcal. gm}^{-1} \cdot \text{C}^{-1}$
- 2) Skeleton - $0.5 \text{ gcal. gm}^{-1} \cdot \text{C}^{-1}$
- 3) All other tissues - $0.9 \text{ gcal. gm}^{-1} \cdot \text{C}^{-1}$

Aschoff and Wever (1) have estimated that the total basal metabolic rate in the resting man can be allocated to the various segments as follows:

TABLE 4

DISTRIBUTION, BY WEIGHT, OF DIFFERENT TISSUE TYPES, OVER THE SIX SEGMENTS, IN % OF TOTAL

	Skin	Fat	Muscle		Core		
			Tela Subcutaneous		Skeleton	Connective Tissue	Viscera Total
	Skin			Muscle			
Head	0.36	0.50		1.00	2.14	0.30	3.0 7.30
Trunk	1.81	9.50		23.59	3.30	4.00	11.0 53.20
Arms	0.65	1.30		4.53	2.02	1.00	9.50
Hands	0.25	0.20		0.10	0.31	0.04	0.90
Legs	1.61	3.20		13.68	6.73	2.58	27.80
Feet	0.32	0.30		0.10	0.50	0.08	1.30
Total	5.00	15.00		43.00	15.00	9.00	14.0 100.00

TABLE 5

C(N), HEAT CAPACITANCE OF COMPARTMENT N, KCAL/DEG C

OLD MODEL

	CORE	MUSCLE	FAT	SKIN
HEAD	3.029	0.675	0.225	0.243
TRUNK	9.465	15.920	4.280	1.222
ARMS	1.260	3.060	0.585	0.440
HANDS	0.143	0.067	0.090	0.168
LEGS	3.992	9.250	1.440	1.088
FEET	0.241	0.067	0.135	0.225
CENTRAL BLOOD	2.25			

NEW MODEL

	CORE	MUSCLE	FAT	SKIN
HEAD	2.570	0.390	0.260	0.280
TRUNK	11.440	18.800	4.940	1.410
ARMS	1.640	3.540	0.670	0.500
HANDS	0.160	0.700	0.100	0.200
LEGS	4.930	10.670	1.660	1.250
FEET	0.270	0.070	0.150	0.260
CENTRAL BLOOD	2.60			

- | | |
|-----------------------------------|--------|
| 1) Brain | - 16 % |
| 2) Trunk core | - 56 % |
| 3) Skin and musculature | - 18 % |
| 4) Skeleton and connective tissue | - 10 % |

They have also reported the resting metabolic rate as $0.3 \text{ kcal/kg}^{-1} \cdot \text{h}^{-1}$ for skin and 0.48 for skeletal muscle.

Basal metabolic rate has been assumed equal to 86.5 kcal.h^{-1} . Based upon the above assumption, a basal heat production ($QB(N)$), has been assigned to each compartment. These values are given in Table 6.

According to Stolwijk (39), basal evaporative heat loss rate $EB(N)$ is about 21 kcal.h^{-1} . This heat loss has been assigned (Table 7) as follows:

<u>Compartment</u>	<u>Kcal.h⁻¹</u>
1) Trunk core	10.45
2) Head skin	0.81
3) Trunk skin	3.78
4) Arms skin	1.40
5) Hands skin	0.52
6) Legs skin	3.32
7) Feet skin	0.72
Total	21.00

The first term accounts for the evaporative heat loss from the respiratory tract. The remaining kcal.h^{-1} assigned to the various skin areas represent vaporization from the skin.

TABLE 6

QB(N), BASAL METABOLIC HEAT PRODUCTION IN N, KCAL/H

OLD MODEL

	CORE	MUSCLE	FAT	SKIN
HEAD	11.200	0.270	0.125	0.061
TRUNK	39.200	6.380	2.341	0.307
ARMS	0.688	1.245	0.325	0.110
HANDS	0.087	0.027	0.050	0.041
LEGS	2.226	3.700	0.800	0.270
FEET	0.145	0.027	0.075	0.054

NEW MODEL

	CORE	MUSCLE	FAT	SKIN
HEAD	14.950	0.120	0.130	0.090
TRUNK	52.600	5.810	2.490	0.470
ARMS	0.820	1.110	0.200	0.150
HANDS	0.090	0.230	0.030	0.060
LEGS	2.590	3.320	0.500	0.370
FEET	0.150	0.020	0.050	0.080

TABLE 7

EB(N), BASAL EVAPORATIVE HEAT LOSS FROM N, KCAL/H

OLD MODEL

	CORE	MUSCLE	FAT	SKIN
HEAD	4.500	0.0	0.0	0.612
TRUNK	4.500	0.0	0.0	3.270
ARMS	0.0	0.0	0.0	1.185
HANDS	0.0	0.0	0.0	0.432
LEGS	0.0	0.0	0.0	2.980
FEET	0.0	0.0	0.0	0.600

NEW MODEL

	CORE	MUSCLE	FAT	SKIN
HEAD	0.0	0.0	0.0	0.810
TRUNK	10.450	0.0	0.0	3.780
ARMS	0.0	0.0	0.0	1.400
HANDS	0.0	0.0	0.0	0.520
LEGS	0.0	0.0	0.0	3.320
FEET	0.0	0.0	0.0	0.720

Table 8 also shows the estimate for basal blood flow, $BFB(N)$, to the various compartments in all six segments. Stolwijk and Hardy (42) have listed the considerations on which the values for blood flow to trunk core and head core have been based. Values for the resting muscle blood flow and the flow to other relatively inactive areas were based on the minimum blood flow required to supply the oxygen requirements for the metabolic rate listed for each area. The hands and the feet possess special circulatory structures and this requires blood flow far in excess of the metabolic requirements, at least in the basal state. The same considerations apply to the assignment of blood flows to the other skin areas. Based upon the assumptions given above, the total cardiac output adds up to 5.2 l/min, which appears reasonable in the light of the aggregate of assumptions made.

Table 9 shows the heat conductances between layers within one segment, $TC(N)$. The calculations for the heat conductances were carried out in the manner indicated by Stolwijk and Hardy (41). Table 9 also shows the intermediate steps. In the calculations shown in Table 9 the head has been considered a sphere. Where feasible, as in the case of the trunk, arms, and legs, the lengths of the segments were measured. For the hands and feet an equivalent cylindrical length and radius were obtained from volume and surface area measurements. $TC(N)$ represents the estimated thermal conductance in $\text{kcal} \cdot \text{h}^{-1} \cdot ^\circ\text{C}^{-1}$ between layer N and layer N+1.

TABLE 8

BFB(N), BASAL EFFECTIVE BLOOD FLOW TO N, LITRES/H

OLD MODEL

	CORE	MUSCLE	FAT	SKIN
HEAD	48.000	0.270	0.120	1.440
TRUNK	232.000	6.400	2.300	2.100
ARMS	0.690	1.240	0.320	0.500
HANDS	0.100	0.050	0.050	2.000
LEGS	2.200	3.700	0.800	2.850
FEET	0.150	0.030	0.080	3.000

NEW MODEL

	CORE	MUSCLE	FAT	SKIN
HEAD	45.000	0.120	0.130	1.440
TRUNK	210.000	6.000	2.560	2.100
ARMS	0.840	1.140	0.200	0.500
HANDS	0.100	0.240	0.040	2.000
LEGS	2.690	3.430	0.520	2.850
FEET	0.160	0.020	0.050	3.000

TABLE 9

ESTIMATION OF THERMAL CONDUCTANCE BETWEEN LAYERS

	Volume Cm ³	Length Cm	Radius Cm	Interface Radius Cm	Cross- section Cm ²	Area Δx	Avg. Cond. Cm ² /cm OC/ Sec x 10 ⁴	TC(N) kcal/ OC · h	
								Old Model	New Model
Head	core	3440	9.37	9.4	1110	1110	10	4.0	1.61
	muscle	4190	10.0	10.2	1305	3250	6.65	7.8	13.25
	fat	4565	10.3	10.4	1370	5480	6.65	13.2	16.10
	skin	4835	10.5						
Trunk	core	11730	7.91	7.91	2960	400	10	1.45	1.59
	muscle	29430	12.52	43.2	4950	1850	8.3	5.55	5.53
	fat	36555	13.95	14.0	5250	6550	6.65	15.7	23.08
	skin	37913	14.19						
Arms	core	2065	2.42	2.42	1690	800	10	2.9	1.4
	muscle	5465	3.94	4.10	2880	3200	8.3	9.6	8.9
	fat	6440	4.28	4.30	3000	12000	6.65	28.8	30.5
	skin	6928	4.43						
Hands	core	262	0.93	0.93	570	1140	10	4.1	6.4
	muscle	337	1.05	1.10	660	4000	6.65	9.6	11.2
	fat	487	1.27	1.40	840	4000	6.65	9.6	11.5
	skin	674	1.49						
Legs	core	6680	3.64	3.64	3640	1450	10	5.25	10.5
	muscle	16955	5.82	6.00	6000	4800	8.3	14.10	14.4
	fat	19355	6.20	6.30	6300	21000	6.65	50.5	74.5
	skin	20563	6.42						
Feet	core	453	1.07	1.07	845	1400	10	5.05	16.3
	muscle	528	1.16	1.20	930	7150	6.65	17.2	20.6
	fat	753	1.38	1.50	1160	5800	6.65	13.9	16.4
	skin	993	1.58						

The overall environmental heat transfer coefficient has been shown in Table 10. Because the segments have different dimensional characteristics, each has a different value for the overall environmental heat transfer coefficient. Using the dimensions adopted in Table 10 and estimated effective radiant surface areas, the calculations for the combined environmental heat transfer coefficients were carried out with the help of conventional methods of heat transfer calculations. The values given in Table 10 are said by Stolwijk to be within ± 5 percent for an ambient temperature range of 10 to 40 $^{\circ}\text{C}$ and for air velocities upto 10 $\text{m}\cdot\text{sec}^{-1}$. The calculated combined coefficients are higher than those found experimentally. The reason for the discrepancies lies in the fact that Stolwijk's experimental values were obtained with the subject wearing shorts and seated on a stool. Both these deviations from the nude standing man tend to reduce the values of both the radiant and convective heat transfer coefficients.

Using the values given in Table 10, we can calculate the combined environmental heat transfer coefficient for any experimental situation. The formula used is:

$$H(I) = (HR(I) + 3.16 * HC(I) * V^{.5}) * S(I)$$

where $H(I)$ - Total environmental heat transfer coefficient for segment
I in $\text{kcal}\cdot\text{h}^{-1}\cdot^{\circ}\text{C}^{-1}$

$HR(I)$ - Radiant heat transfer coefficient for segment I in
 $\text{kcal}\cdot\text{h}^{-1}\cdot\text{m}^{-2}\cdot^{\circ}\text{C}^{-1}$

$HC(I)$ - Convective and conductive heat transfer coefficient
for segment I in $\text{kcal}\cdot\text{h}^{-1}\cdot\text{m}^{-2}\cdot^{\circ}\text{C}^{-1}$

V - Air velocity in $\text{m}\cdot\text{sec}^{-1}$

TABLE 10

CALCULATED COMBINED ENVIRONMENTAL HEAT TRANSFER COEFFICIENT FOR A NUDE MAN, STANDING IN AN ENVIRONMENT WHERE WALL AND AIR TEMPERATURE ARE THE SAME

Segment	Shape	Length cm	Radius cm	Radiant Heat Transfer Coefficient		Convective Heat Transfer Coeff.	Combined Environmental Heat Transfer Coefficient	
				Old Model	New Model		Old Model	New Model
				$\text{kcal} \cdot \text{m}^{-2} \cdot \text{h}^{-1} \cdot \text{C}^{-1}$	$\text{kcal} \cdot \text{m}^{-2} \cdot \text{h}^{-1} \cdot \text{C}^{-1}$	$\text{kcal} \cdot \text{m}^{-2} \cdot \text{h}^{-1} \cdot \text{C}^{-1}$	$\text{kcal} \cdot \text{m}^{-2} \cdot \text{h}^{-1} \cdot \text{C}^{-1}$	$\text{kcal} \cdot \text{m}^{-2} \cdot \text{h}^{-1} \cdot \text{C}^{-1}$
						$v = 0.1 \text{ m} \cdot \text{sec}^{-1}$	$v = \text{Air Velocity in}$	$v = \text{Air Velocity in}$
						$\text{kcal} \cdot \text{m}^{-2} \cdot \text{h}^{-1} \cdot \text{C}^{-1}$	$\text{m} \cdot \text{sec}^{-1}$	$\text{m} \cdot \text{sec}^{-1}$
							$0.1 \text{ m} \cdot \text{sec}^{-1}$	$0.1 \text{ m} \cdot \text{sec}^{-1}$
							Old Model	New Model
Head	Sphere		10.5	5.5	4.8	0.57	0.805	1.350
Trunk	Cyl.	60.0	14.2	4.5	4.8	1.6	4.150	5.269
Arms	Cyl.	112.0	4.4	4.5	4.2	3.4	2.003	1.691
Hands	Cyl.	96.0	1.5	3.0	3.6	5.2	0.775	0.761
Legs	Cyl.	160.0	6.4	4.5	4.2	3.1	4.533	3.787
Feet	Cyl.	125.0	1.6	4.0	4.0	5.1	1.182	1.039

$S(I)$ = Surface area of segment I in m^2

Stolwijk's controlling system

The controlling system represents the thermoregulatory control functions of the autonomic nervous system. It is important to note that the biothermal control system is a negative feedback system with two controlled outputs, namely the mean skin temperature, TS, and the true mean body temperature, TB.

The controller concept is formulated so as to keep the controller as flexible as possible. This approach keeps the number of constraints in the expression of a particular regulator concept to the minimum. Simultaneously, it is possible to add to the formulation without having to make extensive changes in other parts of the model. To accomplish these objectives, the controller is divided into three parts. The first part represents the thermoreceptors. The second part integrates the afferent signals and determines the nature and magnitude of efferent commands. The third part represents the effector mechanisms; the effector commands are distributed and the different effector activities are translated into changes in metabolic heat production, evaporative heat-loss rate, and blood flow for each compartment. Table 11 gives a listing of symbols used in the description of the controlling system.

In the first part of the controlling system, thermoreceptor output is determined. The expression used is:

$$ERROR(N) = T(N) - TSET(N) + RATE(N) * F(N)$$

TABLE 11

DEFINITION OF SYMBOLS USED IN THE DESCRIPTION OF THE CONTROLLING SYSTEM

TSET(N)	"Set point" or threshold temperature for receptors in N	°C
ERROR(N)	Total output signal from receptors in N	°C
RATE(N)	Dynamic sensitivity of receptors in N	hours
COLD(N)	Output from cold receptors in N	°C
WARM(N)	Output from warm receptors in N	°C
COLDS	Total integrated output from skin cold receptors	°C
WARMS	Total integrated output from skin warm receptors	°C
SWEAT	Total efferent sweating command	°C
CHILL	Total efferent shivering command	°C
DILAT	Total efferent vasodilatation command	°C
STRIC	Total efferent vasoconstriction command	°C
SKINR(I)	Relative weight of skin of each segment in determining total skin output	
SKINS(I)	Fraction of sweating command to segment I	
SKINV(I)	Fraction of vasodilatation command to I	
SKINC(I)	Fraction of vasoconstriction command to I	
WORK(I)	Fraction of total exercise occurring in I	
MCHIL(I)	Fraction of total shivering command to I	
CSW	Coefficient for sweating command from head core	
SSW	Coefficient for sweating command from skin	
PSW	Coefficient for sweating command from product of head core and skin	
CDIL	Coefficient for vasodilatation command from head core	
SDIL	Coefficient for vasodilatation command from skin	
PDIL	Coefficient for vasodilatation command from product of head core and skin	
CCON	Coefficient for vasoconstriction command from head core	
SCON	Coefficient for vasoconstriction command from skin	
PCON	Coefficient for vasoconstriction command from product of head core and skin	
CCHIL	Coefficient for shivering command from head core	
SCHIL	Coefficient for shivering command from skin	
PCHIL	Coefficient for shivering command from product of head core and skin	

This equation states that the thermoreceptor output from compartment N is equal to the difference between the instantaneous temperature $T(N)$ and the set-point temperature for that compartment, $TSET(N)$. To this difference is added the product of the dynamic sensitivity factor of the receptors in compartment N ($RATE(N)$) and the rate of temperature change $F(N)$. In the above expression $T(N)$ and $F(N)$ are calculated continuously, and $TSET(N)$ and $RATE(N)$ are constants supplied with the initial conditions. For example, since there seems to be no dynamic sensitivity in the hypothalamic receptors (13), $RATE(1)$, which expresses the dynamic sensitivity of the receptors in the head core, is zero. In the present model, $RATE(N)$ is set equal to zero for all the compartments.

Each of the twenty-five values of $ERROR(N)$ is tested for its sign. Since $ERROR(N)$ terms can become negative as well as positive, each of the commands is protected against becoming negative. If $ERROR(N)$ has a positive value, we assume that it represents a warm-receptor output; if negative, it indicates an output from cold receptors. When $ERROR(N)$ is positive, its value is assigned to $WARM(N)$; when it is negative, its absolute value is entered under $COLD(N)$. The resulting lists of $WARM(N)$ and $COLD(N)$ represent all possible afferent thermal information potentially available to the controlling system. We will limit discussion for the present to assumed thermal receptors in the head core and in the skin.

The total warm receptor output from the skin $WARMS$ can be obtained by summing $SKINR(I)*WARM(4*I)$ for the skin compartments of all six segments. The total cold receptor output from the skin can be integrated from a similar summation. If it is desired to take other possible

thermoreceptors into account, they can also be integrated by similar processes.

Next, the type and magnitude of effector command signals which go out to the periphery is determined. These effector commands are SWEAT, DILAT, STRIC, and CHILL for sweating, vasodilation, vasoconstriction, and shivering respectively. Two possible types of integration of afferent signals are being considered here: integration by linear addition of central and peripheral receptors which expresses the concept of the adjustable set point (19), and integration by multiplication of central and peripheral receptor outputs which expresses the gain control concept (22,42). The expression for efferent sweating command then becomes

$$\text{SWEAT} = \text{CSW} * \text{ERROR}(1) + \text{SSW} * (\text{WARMS} - \text{COLDS}) + \text{PSW} * \text{ERROR}(1) * (\text{WARMS} - \text{COLDS})$$

in which ERROR(1), WARMS, and COLDS are thermoreceptor outputs continuously generated by the model, and in which CSW, SSW, and PSW are supplied as controller constants. If CSW and SSW are set to zero, and PSW has a distinct value, the controller has gain control characteristics as outlined in Hardy and Stolwijk (22). If, on the other hand, PSW is zero and CSW and SSW have non-zero values, the controller has adjustable set point characteristics as outlined in Hammel et al (19). Similarly, the expressions for DILAT, STRIC, and CHILL are obtained using the procedure outlined above, and are shown below

$$\text{DILAT} = \text{CDIL} * \text{ERROR}(1) + \text{SDIL} * (\text{WARMS} - \text{COLDS}) + \text{PDIL} + \text{WARM}(1) * \text{WARMS}$$

$$\text{STRIC} = -\text{CCON} * \text{ERROR}(1) - \text{SCON} * (\text{WARMS} - \text{COLDS}) + \text{PCON} * \text{COLD}(1) * \text{COLDS}$$

$$\text{CHILL} = (\text{CCHIL} * \text{ERROR}(1) + \text{SCHIL} * (\text{WARMS} - \text{COLDS})) * \text{PCHIL} * (\text{WARMS} - \text{COLDS})$$

The values for the controller constants were supplied by Stolwijk (39).

The next step consists of the estimation of effector actions in the various compartments in each segment. The effector actions are $BF(N)$, $Q(N)$, and $E(N)$ and the process of estimating their values is best done by segment, each segment consisting of four distinct layers. The subscript N refers to the core of a segment, $N+1$ refers to the muscle layer; $N+2$ to the subcutaneous fat, and $N+3$ to the skin layer. The metabolic heat production in each layer of a segment can be expressed as

$$\text{core}---Q(N)=QB(N)$$

$$\text{muscle}---Q(N+1)=QB(N+1)+WORKM(I)*WORK+CHILM(I)*CHILL$$

$$\text{fat}----Q(N+2)=QB(N+2)$$

$$\text{skin}---Q(N+3)=QB(N+3)$$

According to the first expression, metabolic heat production in the core of each cylinder always remains at the basal level. This is not strictly true for the trunk where the heat produced by the heart is especially variable, but the thermal error introduced by inserting this heat into working skeletal muscle instead of into the trunk core is quite small. The heat production in the brain is quite constant, and in the extremities the heat production in the core is low under all circumstances. Heat produced in the musculature consists of the basal production plus the fraction of total shivering assigned to the segment. Both of these fractions are introduced with the initial conditions.

The blood flow to the core of each segment is considered a constant and equal to the basal blood flow:

$$BF(N)=BFB(N)$$

As a first approximation, we can consider muscle blood flow to consist

of the basal blood flow, to which we can add $1 \text{ litre} \cdot \text{h}^{-1}$ for each $\text{kcal} \cdot \text{h}^{-1}$ of heat production due to work, or shivering by the muscular compartment in question. Thus,

$$\text{BF}(N+1) = \text{BFB}(N+1) + Q(N+1) - Q_B(N+1)$$

Blood flow in the subcutaneous fat has a low basal level, and as a first approximation it is not considered to vary as a result of thermoregulatory responses:

$$\text{BF}(N+1) = \text{BFB}(N+3)$$

Skin blood flow is highly dependent on the thermoregulatory controller. The basal blood flow at thermal neutrality can be diminished by vasoconstriction or increased by vasodilation. These adjustments are accompanied by changes in the peripheral resistance. The sensitivity of different skin areas is sufficiently different to require special terms as shown in the expression:

$$\text{BF}(N) = (\text{BFB}(N) + \text{SKINV}(I) * \text{DILAT}) / (1 + \text{SKINC}(I) * \text{STRIC})$$

$\text{SKINV}(I)$ and $\text{SKINC}(I)$ represent the relative responsivity of the skin of different segments and are supplied with the controller constants. The controller can add to the basal skin blood flow, or the basal blood flow can be reduced by dividing it by a number determined by the controller. This expression allows for special skin regions such as on the hands and the feet which are highly responsive to both vasodilation and vasoconstriction and other less responsive regions such as the trunk skin with a response largely limited to vasodilation.

Evaporative heat loss occurs from the trunk core and from each of the skin areas. Evaporation from the trunk core is via respiration. Although it depends to some extent on the vapor pressure in the inspired

air, it is here considered a constant at rest. During exercise when a higher respiratory minute volume occurs an average value of respiratory water vapor loss is about 8 percent of the increased metabolic heat production in total. All of this loss is assigned to the heat flow in the central blood.

The response to sweating stimulation is different in different skin areas. In order to allow for this difference, the efferent command is multiplied with a factor $SKINS(I)$ for each segment. According to Bullard et al (10) the local temperature of the skin has a modifying influence on the local sweat secretion in response to a given level of efferent commands. The following expression, as a first approximation, incorporates the above requirements:

$$E(N+3) = EB(N+3) + SKINS(I) * SWEAT * 2.^{((T(N+3) - TSET(N+3))/4.)}$$

The term $SKINS(I) * SWEAT$ includes the responsiveness of the skin area of segment I and the efferent sweating command signal. This term is then multiplied by another term $2.^{((T(N+3) - TSET(N+3))/4.)}$. If the local skin temperature is at the undisturbed thermally neutral level, the latter term then becomes equal to 1. For every four-degree rise in local skin temperature, the value of this term doubles; and for every four-degree fall in local skin temperature, the local sweat secretion is reduced to half. This is, of course, only an approximation of the findings of Bullard et al, but over normal physiological ranges the deviation from their curves is not very great.

Unless special precautions are taken, $E(4*I)$ the rate of evaporative heat loss from the skin of segment I, could assume values dictated by the

controller which are physically impossible due to high ambient water vapor pressure. This can be checked by determining the maximum rate of evaporative heat loss possible from segment I. The following expression will compute EMAX:

$$\text{EMAX(I)} = (\text{PSKIN} - \text{PAIR}) * 2.14 * (\text{H(I)} - \text{HR(I)} * \text{S(I)})$$

PSKIN and PAIR are the water vapor pressure at the skin surface and in the environment in mm Hg; $2.14 * (\text{H(I)} - \text{HR(I)} * \text{S(I)})$ is the product of a surface area and a coefficient for evaporative power as found by Brebner et al (8). If E(4*I) in any skin area exceeds EMAX(I), then it must be reduced to EMAX(I). Note that the ratio $\text{E(4*I)} / \text{EMAX(I)}$ for each segment gives the fractional wetted area.

There is a very small amount of direct information concerning the values of SKINR, SKINS, SKINV, SKINC, WORKM, and CHILM. The simplest approach would be to insert values which are proportional to the surface areas or the weights of the different tissues. These weights and proportions are shown in Table 12 for skin and muscle layers. There is reason to adopt the relative sensitivities and numbers of skin receptors proposed by Aschoff and Wever (1). The factual basis for these values is somewhat obscure. Bader and Macht (2) show a relatively higher sensitivity in head and chest than in the extremities, but there is reason to suspect that in their case the heat applied to the skin was sensed by deeper thermoreceptors after having warmed the blood.

It is quite clear that the trunk skin plays a more than proportionate role in skin thermoreception as evidenced by the difference in response to a uniform skin temperature and to an identical average skin temperature with divergent local temperatures.

Hertzman and Randall (24) surveyed the skin with respect to local blood flow. Although their measurements were photoelectric and consequently hard to quantitate, the relative proportions can probably be accepted. After rearrangement, the following fractions of the total blood flow are obtained for the basal and maximally dilated state respectively: head 0.288 and 0.132, trunk 0.265 and 0.322, arms 0.078 and 0.095, hands 0.10 and 0.122, legs 0.186 and 0.23, and feet 0.083 and 0.10.

The fractions for the maximally dilated state are taken as the distribution of vasodilation over the skin, SKINV(I), in Table 12. Vasoconstriction is also not uniform over the skin area. Also, the effects of counter current heat exchange will tend to exaggerate the effects of vasoconstriction in the distal extremities. On the other hand, counter current heat exchange is not so pronounced in the skin of the head and the trunk. Based on this, the assignment of SKINC(I) are made as shown in Table 12.

The relative distribution of sweat secretion in the absence of information based on local secretion measurements is perhaps best approximated by the distribution of sweat glands. Randall (34) made such observations and the different skin areas were weighted as to the number of sweat glands, and the fractional distribution is given as SKINS(I) in Table 12.

Measurements and Procedures

The 18 sessions took place in the KSU-ASHRAE large climatic chamber during the summer of 1972. The subject read a pocketbook or dozed while sitting on a stool which was placed in a tub with mineral oil. The tub plus subject were on a platform scale in the chamber. Any sweat that did

TABLE 12

TENTATIVE ESTIMATES OF DISTRIBUTION OF SENSORY INPUT, EFFECTOR OUTPUT OVER THE SKIN AND OF HEAT PRODUCTION IN MUSCLE DURING WORK AND SHIVERING

	Surface Area		SKINR (I)	SKINS (I)	SKINC (I)	SKINV (I)	Muscle Layer		WORKM (I)	CHILM (I)
	$\frac{m^2}{m}$	%					kg	%		
Head	0.1283	7.00	0.0827	0.081	0.05	0.132	0.750	2.325	—	0.02330
Trunk	0.6850	36.02	0.5870	0.482	0.15	0.322	17.700	54.800	0.30	0.54800
Arms	0.2480	13.41	0.0822	0.154	0.05	0.095	3.400	10.530	0.08	0.10530
Hands	0.0904	5.00	0.2215	0.031	0.35	0.122	0.075	0.233	0.01	0.00233
Legs	0.6240	31.74	0.1860	0.219	0.05	0.230	10.275	31.900	0.60	0.31900
Feet	0.2530	6.86	0.0399	0.035	0.35	0.100	0.075	0.233	0.01	0.00233

not evaporate but dripped off him went below the film of oil. Thus by weighing the tub, the clothing and the nude subject before and after the experiment, we were able to measure evaporation as well as weight loss. Weighings during the experiment permitted estimation of the combined rate of evaporation of dry ice and water. In addition, the 12 chunks of dry ice were weighed and dimensions measured approximately ten minutes before entry to the chamber and ten minutes after departure.

Depending on the session, YSI 409 thermistors were attached to 15 to 31 skin locations. In all sessions, one sensor was on the head below the ear, one on the right upper arm, one on the right calf and one on the right thigh. Rectal temperature was sensed by a YSI rectal probe. Temperatures were recorded every ten minutes with a Digitec digital thermometer and printer.

Every 20 minutes the EKG was recorded for approximately one minute; a count of the r waves for a 30 second period was used to determine heart rate. The subject, a graduate student in physiology, took his blood pressure every 20 minutes. Air velocity normally was low (0.1 m/s). For the higher velocity (0.4 m/s), a large fan 25 feet away produced a turbulent breeze. With the fan on, it was turbulent with a mean velocity of 0.2 m/s on the left side and in front of the subject and 0.5 m/s on the right side and in back. Velocity was measured with a Velometer for the higher velocity and a DISA D5580 low velocity anemometer for the low velocities. The CO₂ concentration was measured with a Bendix-Unico 400 Precision Gas Detector.

For each session the subject was weighed and thermistors taped on various locations. The ice jacket was then put on and the pockets held against the body with an EKG strap. He then entered the chamber at approximately 9:30 a.m., sat on the stool and was weighed while heart rate

and temperatures were recorded. He then took his blood pressure. Temperatures were recorded every ten minutes and weights, heart rate and blood pressure were recorded every 20 minutes. He normally remained 120 minutes although some tests were for 100 or 240 minutes. All environments were $43.3 (+0.6)^{\circ}\text{C}$ dry bulb, with the mean radiant temperature at $42.8 (+1.2)^{\circ}\text{C}$. (Wall and air temperatures are controlled independently in this chamber; the difference was due to an error in the settings for the initial experiments which we continued for consistency.) The relative humidity was either 45 or 55% (vapor pressures of 29.7 or 36.3 mm Hg).

RESULTS

Nude man

For the purpose of validating/updating the Stolwijk model, the data from experiments carried out by Konz et al (27) was compared with predicted response from the model. Simulations were carried out 1) for a nude man and 2) for a man wearing a dry ice vest. We started by using the Stolwijk model presented in 1970 (38) but in the middle of this study we obtained a copy of Stolwijk's new model (39) in which the input data was drastically different from the input data in the earlier model. While the new model gave better results vis a vis our experiments, it was decided to compare results from the two Stolwijk models for bringing out the differences in their predictive capabilities. Thus all the figures showing the comparison between the experimental and simulation results and incorporated in this study show the output from both the original and the new Stolwijk model. The differences between the input values in the old model and those in the new model are substantial. For instance, HC(2), representing the convective heat transfer coefficient for the head, has a value of 0.57 in the old model whereas it is assigned the value 3.00 in the new model. Similar differences are present in most of the other input variables.

The experimental data for the nude man pertains to the three control days viz. July 5, July 24, and July 31. The experimental temperatures were recorded for the following locations: 1) rectal 2) head skin 3) trunk skin 4) arm skin 5) leg skin. In addition, heart rate and blood pressure and sweat rate were measured on all three days. The model output consisted of 1) trunk core temperature 2) head skin

temperature 3) trunk skin temperature 4) arm skin temperature 5) leg skin temperature 6) sweat rate and 7) cardiac output.

Trunk core temperature from the model was compared with the measured rectal temperature as rectal temperature was taken to be representative of the trunk core temperature. Figure 4 shows the experimental rectal temperatures for the three control days plotted along with the simulated temperatures for the trunk core. Figure 4 shows the comparison between the experimental rectal temperature and the simulated trunk core temperature. For the purposes of input to the model at time zero, the average of the three control days' temperatures at time -10 was used (-10 was used to represent the temperatures of the subject in the pre-test chamber). The input to the model for the trunk core was 36.59 C. Both the old and the new simulations seem to fit the experimental data pretty well. In the experimental data, the rectal temperature rose from an average of 36.6 C to 37.3 C over a 120 minute period. The simulated temperature for the trunk core (new model) showed a rise from 36.6 C to 37.3 C over the same period. Thus there seems to be a close fit between simulated and experimental temperatures for the trunk core.

Figure 5 shows the head skin temperatures. In the experimental results, there was a sharp rise in the head skin temperature during the first 20 minutes and then there was a steady drop probably indicating the benefit of sweat loss from the head skin. On an average, the head skin temperature rose from 33.8 C to 37.3 C in the first 20 minutes and then there was a decline down to around 36 C at the end of the 120 minutes.

X July 5
 Δ July 24
 X July 31

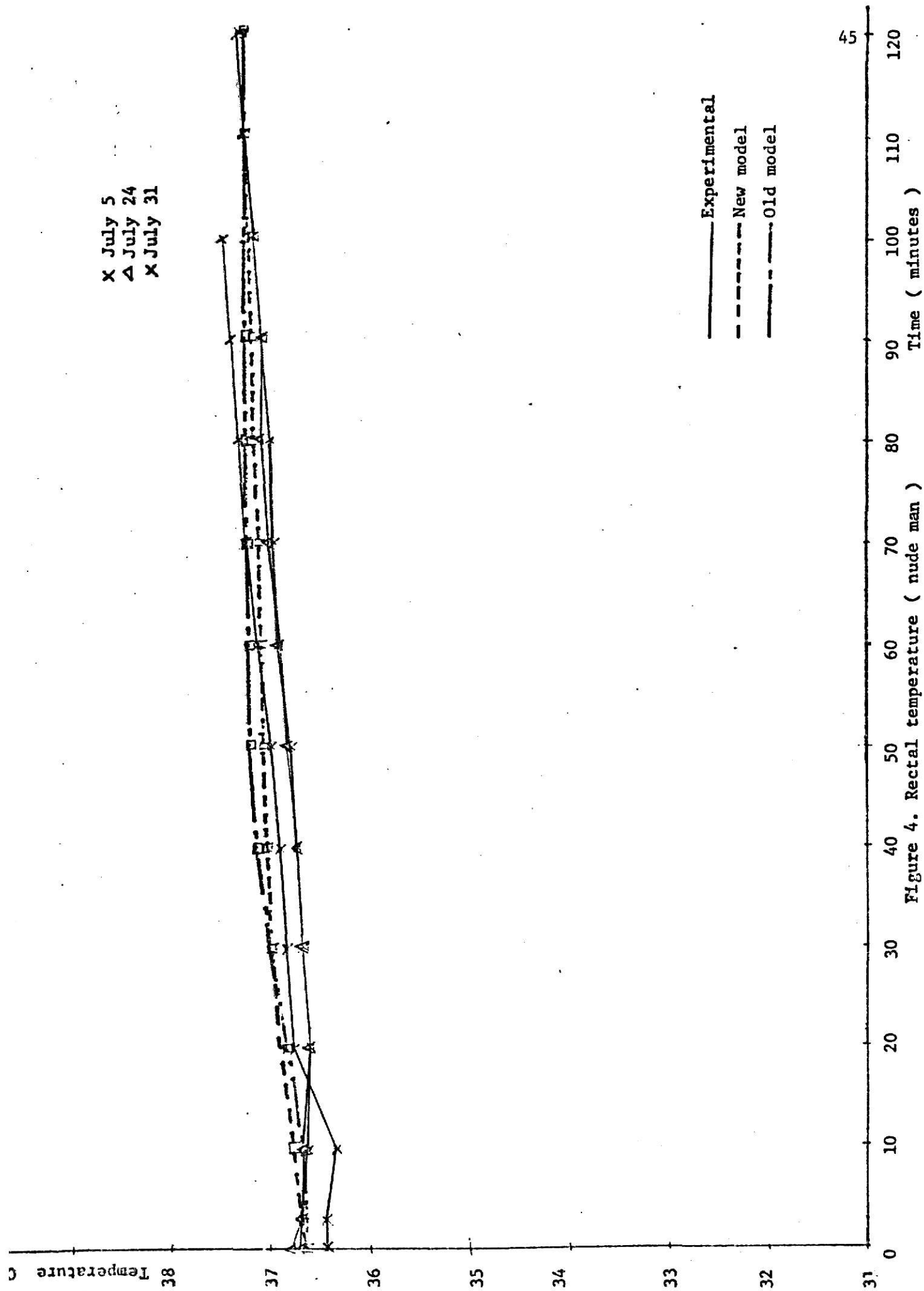
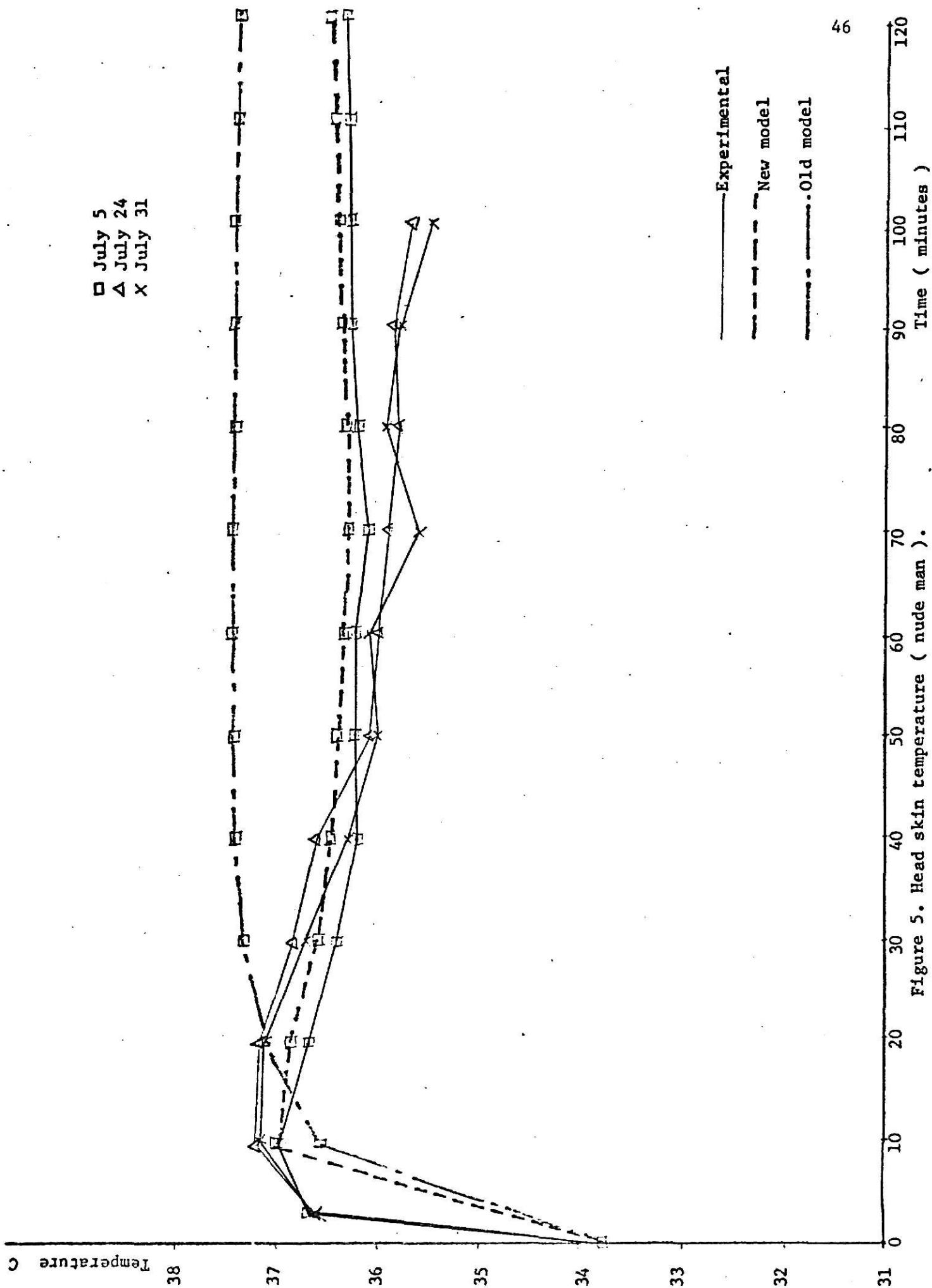


Figure 4. Rectal temperature (nude man)



In the simulation with the original Stolwijk model, the head skin temperature rose steadily from 33.8 C to 37.4 C at the end of the 120 minute and never showed any drop in the intervening period. However, with the new model there was a drop in the head skin temperature after a sharp rise in the first 20 minutes. The head skin temperature from the new model seemed to sit well in the middle of the experimental data.

Trunk skin temperatures are plotted in Figure 6. In the experiments, there were twelve sensors taped on the torso of the subject at various locations and the plotted values represent the average of the twelve readings. The trunk skin temperature in the experimental data shows a rise from an average starting value of 31.7 C to about 37.1 C at the end of the 120 minutes. The two simulation results from the old and new Stolwijk models show a rise in the trunk skin temperature to 36.5 C, thus indicating a difference of about 0.5 C between the simulated and the experimental temperatures for the trunk skin. However, there seems to be reason to accept the experimental values for the trunk skin temperature as more valid since they represent the average of twelve readings. Thus the predicted values for the trunk skin temperature from the two models are about 0.5 C lower than the experimental results.

Figure 7 shows the arm skin temperature. The experimental values range from an average of 31.5 C at 0 minute to 37 C at 120 minutes. The old model showed a rise in the arm skin temperature to about 35.5 C at 120 minutes. In the new model, the arm skin temperature rose to 36.3 C during the same time. Thus the predicted results for the arm skin temperature from both the models are lower than the experimental values

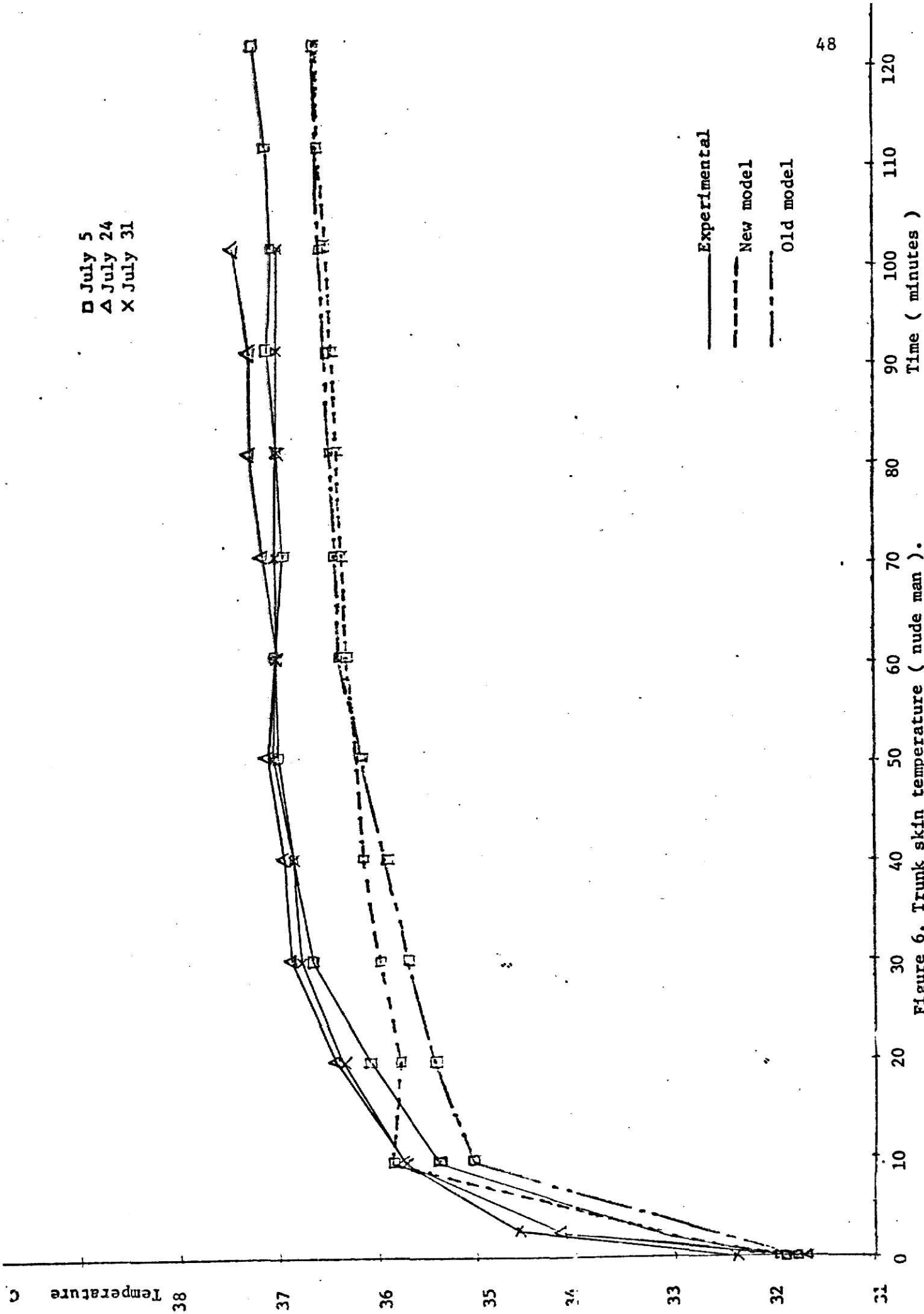


Figure 6. Trunk skin temperature (nude man).

Temperature

38

37

36

35

34

33

32

31

□ July 5
△ July 24
x July 31

Experimental
New model
Old model

49

0

10

20

30

40

50

60

70

80

90

100

110

120

Figure 7. Arm skin temperature (nude man).

Time (minutes)

by 1.5 C and 0.7 C. However, it should be pointed out that there was only one thermistor taped to the arm during the three control days. Considering the wide variations in the skin temperatures of the human body even over relatively small areas, it is still open to question whether the one temperature reading from the arm skin gives the true arm skin temperature. If we assume that the experimental temperature for the arm skin is the true arm skin temperature, the new model is closer to reality than the old model.

The comparison between the experimental leg skin temperature and its simulated counterpart is shown in Figure 8. For the plot representing the experimental leg skin temperature, the mean of calf and thigh temperatures was used. On July 5, the leg skin temperature rose from 32 C to 35.8 C over 90 minutes while on July 24 and July 31 this temperature rose to about 37 C over 120 minutes. Thus it is apparent that there is a wide variation in the temperatures of the same segment of the same human body over different days. This variation may be due to various physiological factors as well as dietary factors. It has been reported that the body temperature of a subject may be lower on a day if the subject had consumed alcoholic beverages on the previous night. While this difference points out the natural variability of human beings as well as the difficulty of replicating even the same subject over different periods of time, at the same time the inherent limitation of a model becomes apparent. The model has no built-in mechanism for taking into account this natural variability of human subjects. Despite this shortcoming of the model, we can compare the

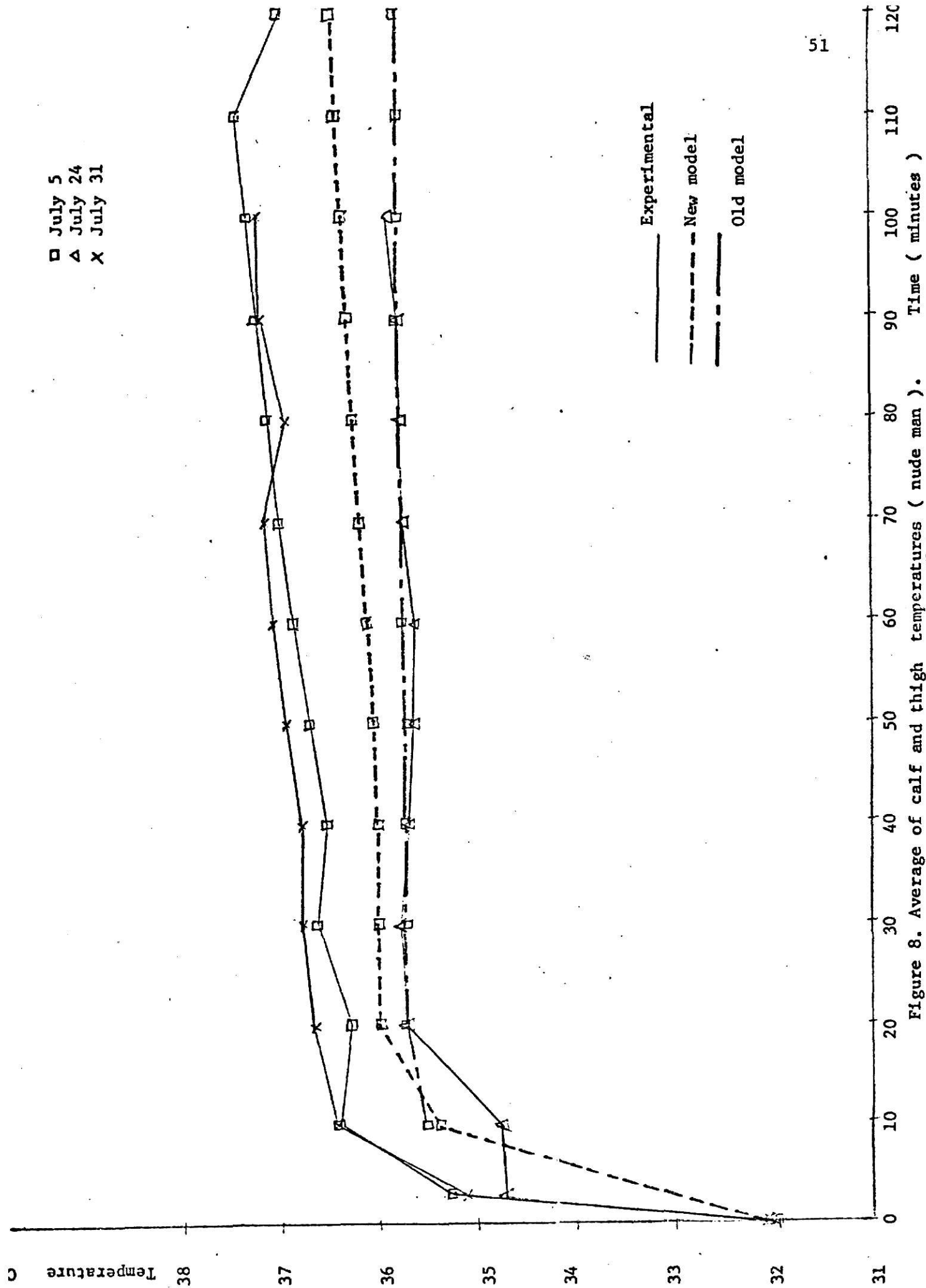


Figure 8. Average of calf and thigh temperatures (nude man).

simulated response with the experimental data. For the leg skin segment the predicted temperature from the old model rises to about 35.7 C while in the new simulation the leg skin temperature rises to about 35.5 C. Thus the new simulation gives a better fit with the experimental data in the case of the leg skin temperature.

Heart rate and systolic blood pressure measurements had been taken on the subject. For making a guesstimate of cardiac output of the subject, heart rate (HR) and systolic blood pressure (SBP) were multiplied together and the resulting term was plotted as a percentage; e.g. value of this term at 0 minute was taken to be 100% and all the succeeding values up to 120 minutes were expressed as a percentage of the initial value. In Figure 9 this term (HR*SBP) was compared with CO, litres/minute, the cardiac output given by the model. CO was also plotted as a percentage. The simulated value of CO rose 33% over 120 minutes in the new model whereas in the old model the rise was only 7%. HR*SBP value increased 36% on an average over the same period. While it cannot be stated with any certainty that the HR*SBP term represents the true cardiac output of the subject, it is used here strictly for the purpose of comparison with CO.

Two points will be made here. First, cardiac output for the new model is substantially higher than for the old. Second, the basic equations for CO are the same in the two models. Basal blood flow for the skin is the same for both models and changed slightly (maximum .4 litres/h) for fat and muscle. Trunk core blood flow was increased to 232 litres/h from 210. QB(basal metabolism) was increased from 70 kcal/h to 86.5. The equation for the skin blood flow has been

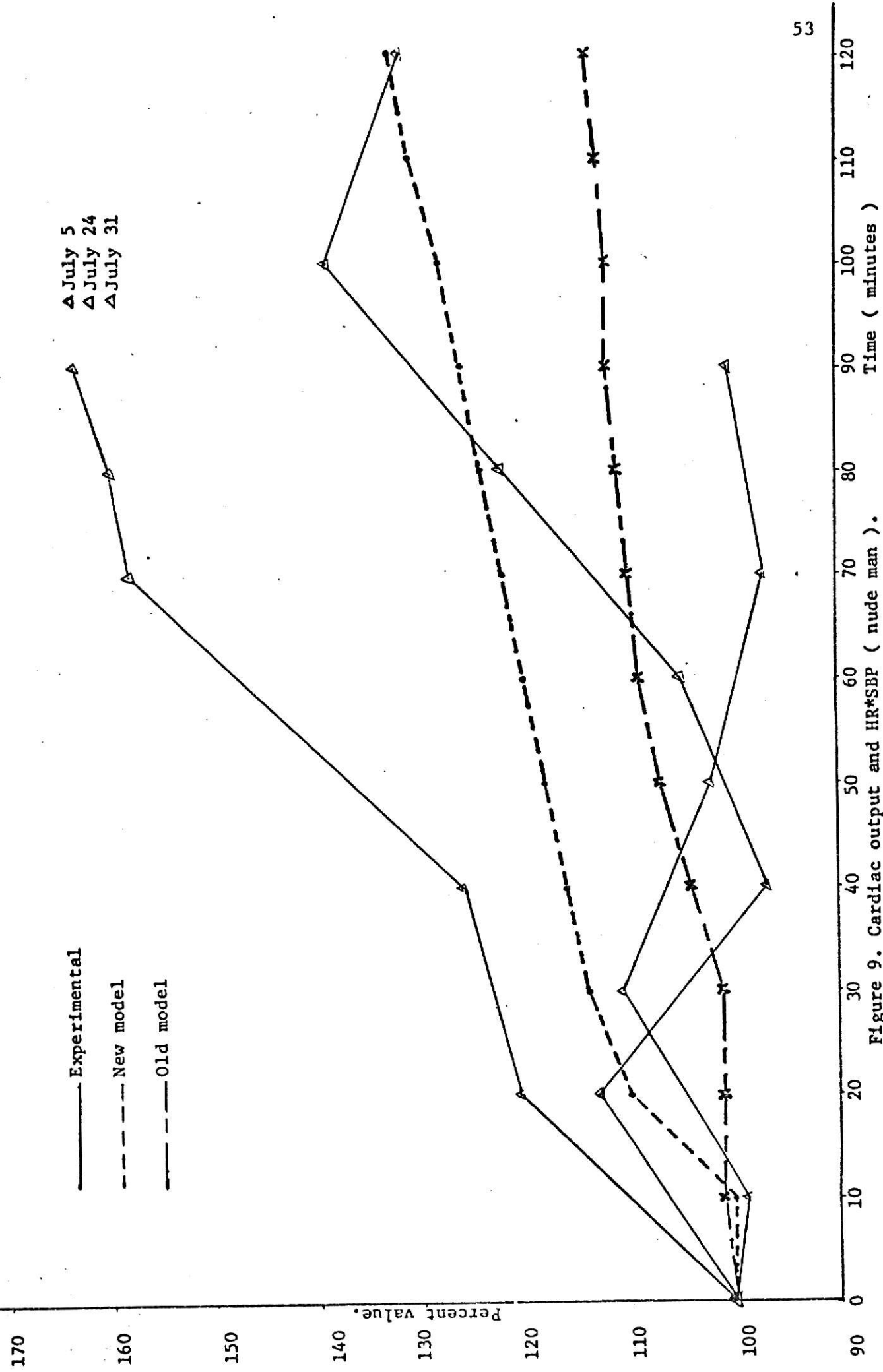


Figure 9. Cardiac output and HR*SBP (nude man).

modified by changing the DILAT equations' coefficients so that skin blood flow at 120 minutes increased from 50 litres/h to 102.

Figure 10 shows the plots for the required sweat loss calculated from the heat balance equation from the experimental data (EVAPR) and the predicted value for evaporative heat loss given by the model (EV). EVAPR rose from 0 kcal/h at minute 0 to 152 at minute 120. In the new model EV rose from 21 kcal/h at 0 minutes to 166 at 120 minutes whereas in the old model this rise was from 18 to 158. The two models seem to be reasonably similar to each other and both give a reasonably good prediction of the experimental data for evaporative sweat loss.

Dry ice vest

Stolwijk's model in its existing form is applicable to a nude man only; we had to modify the model to make it applicable to a man wearing a dry ice vest.

For the dry ice cooling we had to make the best estimate for the combined environmental heat transfer coefficient for the trunk segment (the vest covered only the trunk portion of the subject). To incorporate the effect of cooling provided by the dry ice vest into the model, the sublimation rate of dry ice was used. Although actual sublimation varied greatly with time, the simulation assumes constant sublimation during the experiment. Each kg of sublimed dry ice was assumed to provide a cooling benefit of 137 kcal/h. The benefit provided by the gas temperature rise was taken care of in $H(2)$, the combined environmental heat transfer coefficient for the trunk segment. DWC_{O2} , the rate of sublimation of dry ice in kg/h, was multiplied by 137 kcal/kg and a factor K . K accounted

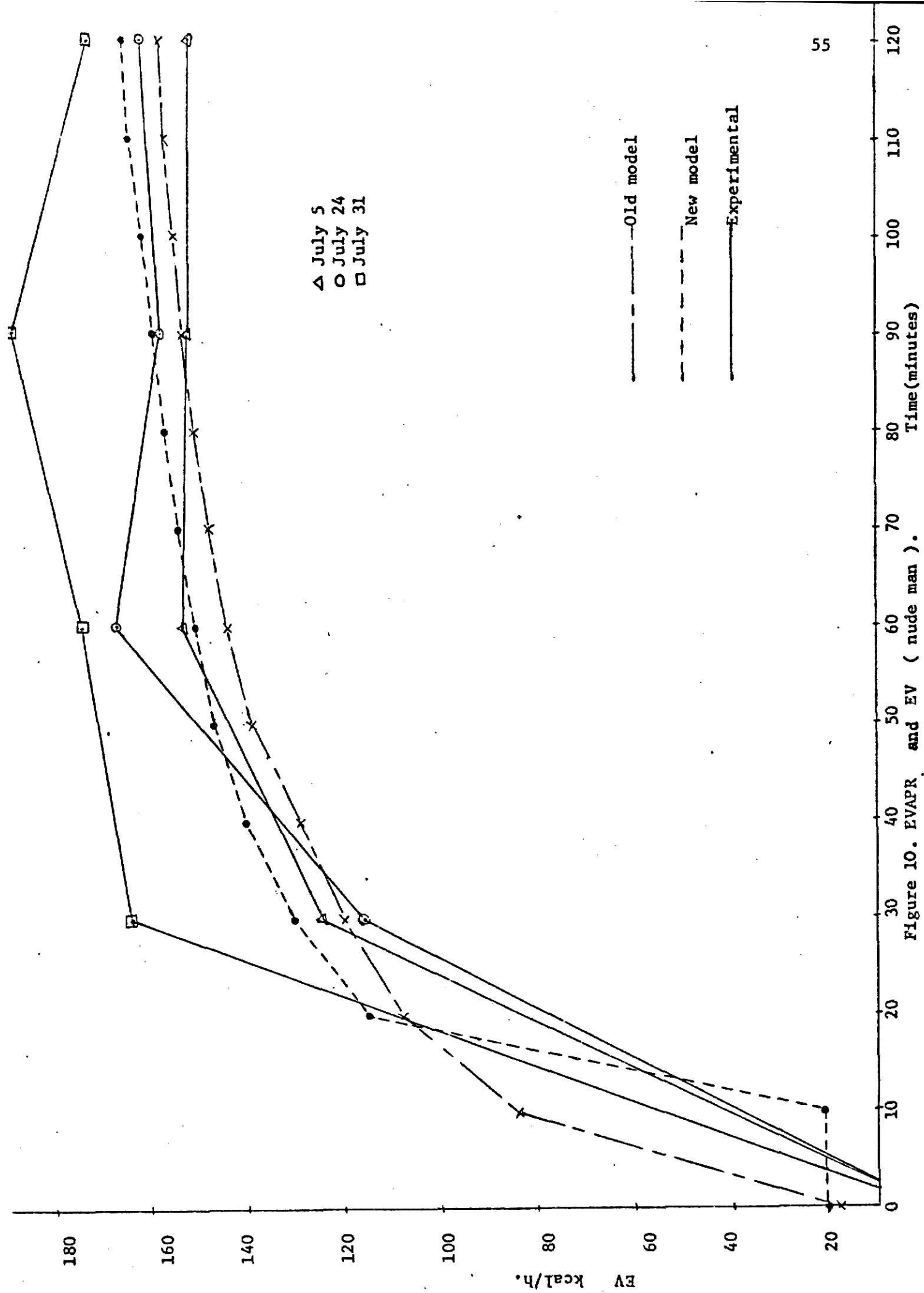


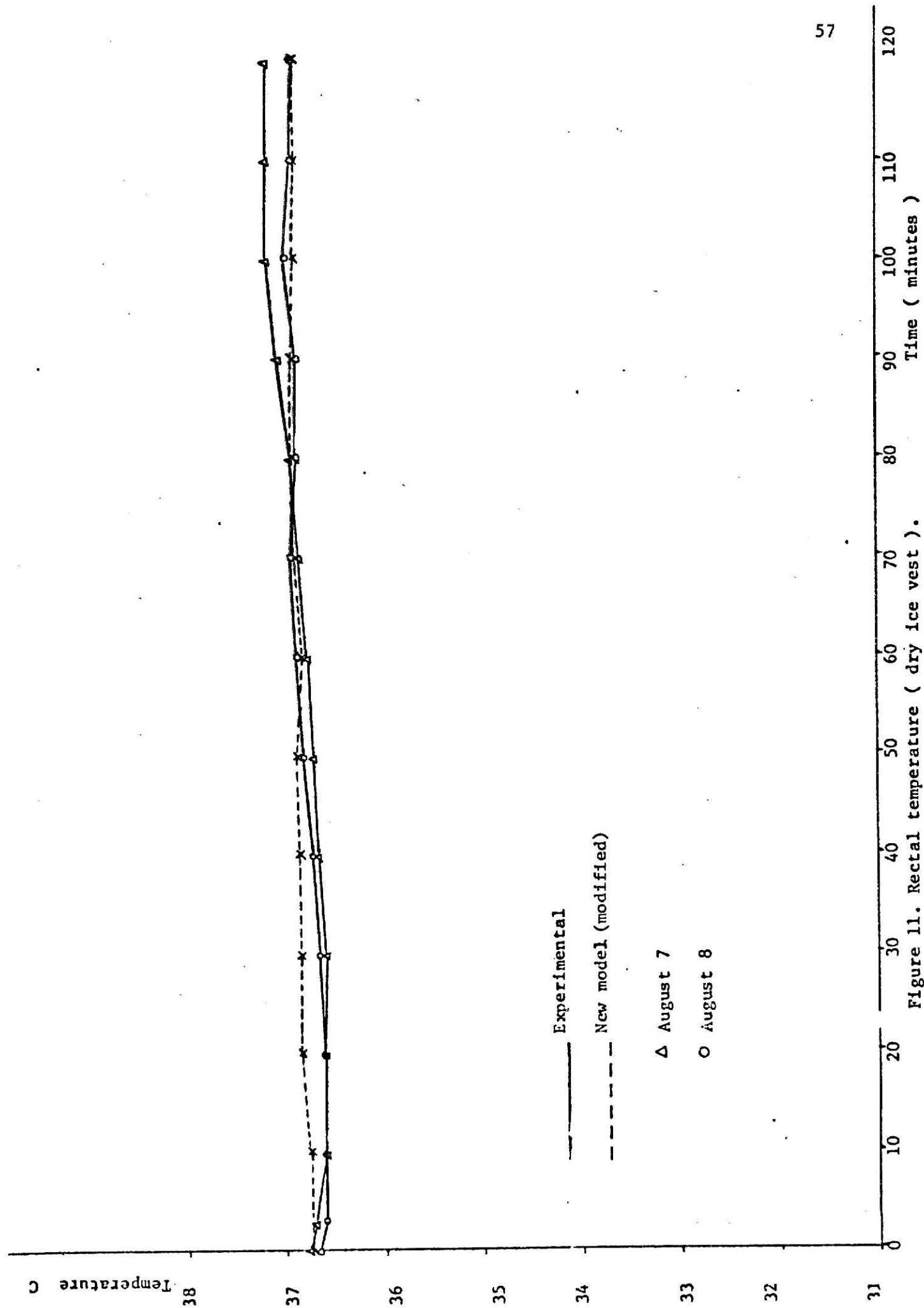
Figure 10. EVAPR and EV (nude man).

for the fraction of heat provided by the body of the subject towards the sublimation of dry ice; $(1-K)$ came from the environment. The modified equation for heat balance in the trunk skin segment after taking into account the effect of dry ice cooling was as follows:

$$HF(8) = Q(8) - BC(8) - E(8) + TD(7) - H(2) * (T(8) - TAIR(2)) - SUBLM$$

where $SUBLM = DWCO_2 * 137.0 * K$. In Stolwijk's old model, TAIR had the same value for all the six segments; we used TAIR as a variable to account for possible differences in radiant temperatures facing different body segments. $H(2)$ had a value of 5.27 in Stolwijk's new model. The experimental trunk skin temperature $(.14T_p + .86T_{np})$ where T_p = temperature under a dry ice pocket and T_{np} = temperature on unaffected trunk skin) was plotted for August 7 and 8th. Then the simulated trunk skin temperature was plotted using different values of $H(2)$. A good fit between the simulated and experimental results for the trunk skin temperature was obtained for $H(2) = 1.1$ kcal/h/C. To obtain a reasonable value for K , plots of simulated trunk skin temperature were made using different values of K while $H(2)$ was held constant at 1.1. From these plots we obtained a value of 0.7 for K which seemed to give a good fit between the simulated and experimental trunk skin temperatures.

Figures 11 to 17 refer to the dry ice vest simulations. Figure 11 shows the experimental rectal temperatures for August 7 and 8 plotted along with the simulated trunk core temperature. For the purposes of input to the model at time zero, the average of the two days' (August 7 and 8) temperatures at time -10 was used. The input to the model for the trunk core was 36.73 C. The simulation seems to fit the experimental



data pretty well. In the experimental data, the rectal temperature rose from an average of 36.73 C to 37.2 C over a 120 minute period. The simulated temperature for the trunk core showed a rise from 36.73 C to 37 C over the same period.

Figure 12 shows the head skin temperature. In the experimental results, there was a sharp rise in the head skin temperature during the first 20 minutes and then there was a steady drop. On an average, the head skin temperature rose from 33.53 C to 37.2 C in the first 30 minutes and then there was a decline to around 36.5 C at the end of 120 minutes. The simulated head skin temperature rose sharply from 33.53 C to 37.6 C in the first twenty minutes and then declined to 36.9 C at 120 minutes, thus indicating a good fit to the experimental data.

Trunk skin temperatures are plotted in Figures 13 and 14. In the experiments, there were twelve sensors placed under the dry ice pockets and one sensor was placed on the trunk skin region unaffected by the cooling. The trunk skin temperature (weighted average) was estimated as shown before ($.14T_p + .86T_{np}$). The estimated experimental trunk skin temperature showed a rise from an average starting value of 31.12 C to about 33.8 C at the end of 120 minutes. Figure 13 shows two simulation lines for the trunk skin temperature with different K values. Similarly, Figure 14 shows two simulation lines for the trunk skin temperature with different $H(2)$ values. The simulation lines in Figs. 13 and 14 are intended to show the effect of changing K and $H(2)$ on the model output. By comparing Figures 13 and 14 it is apparent that a

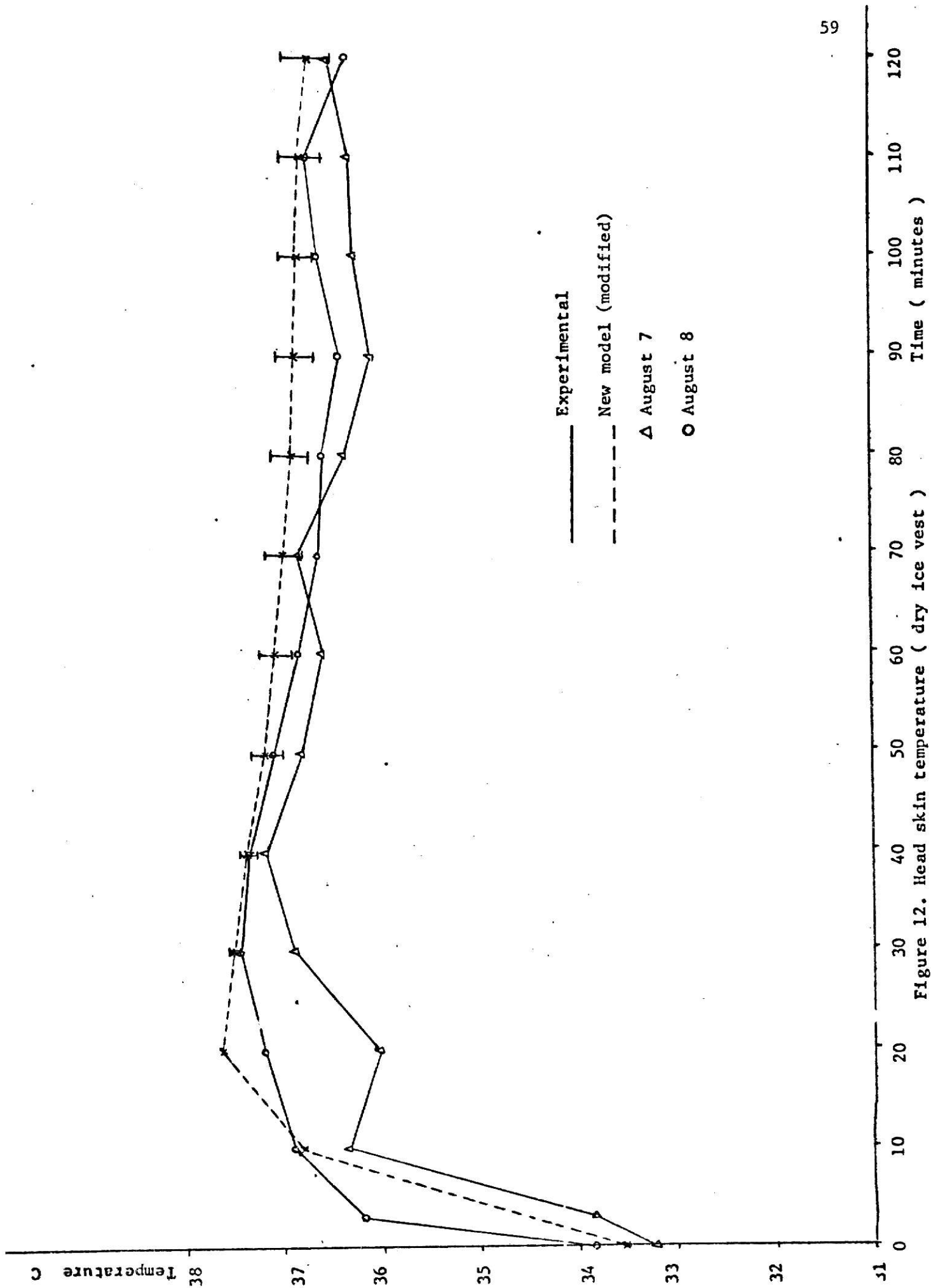


Figure 12. Head skin temperature (dry ice vest)

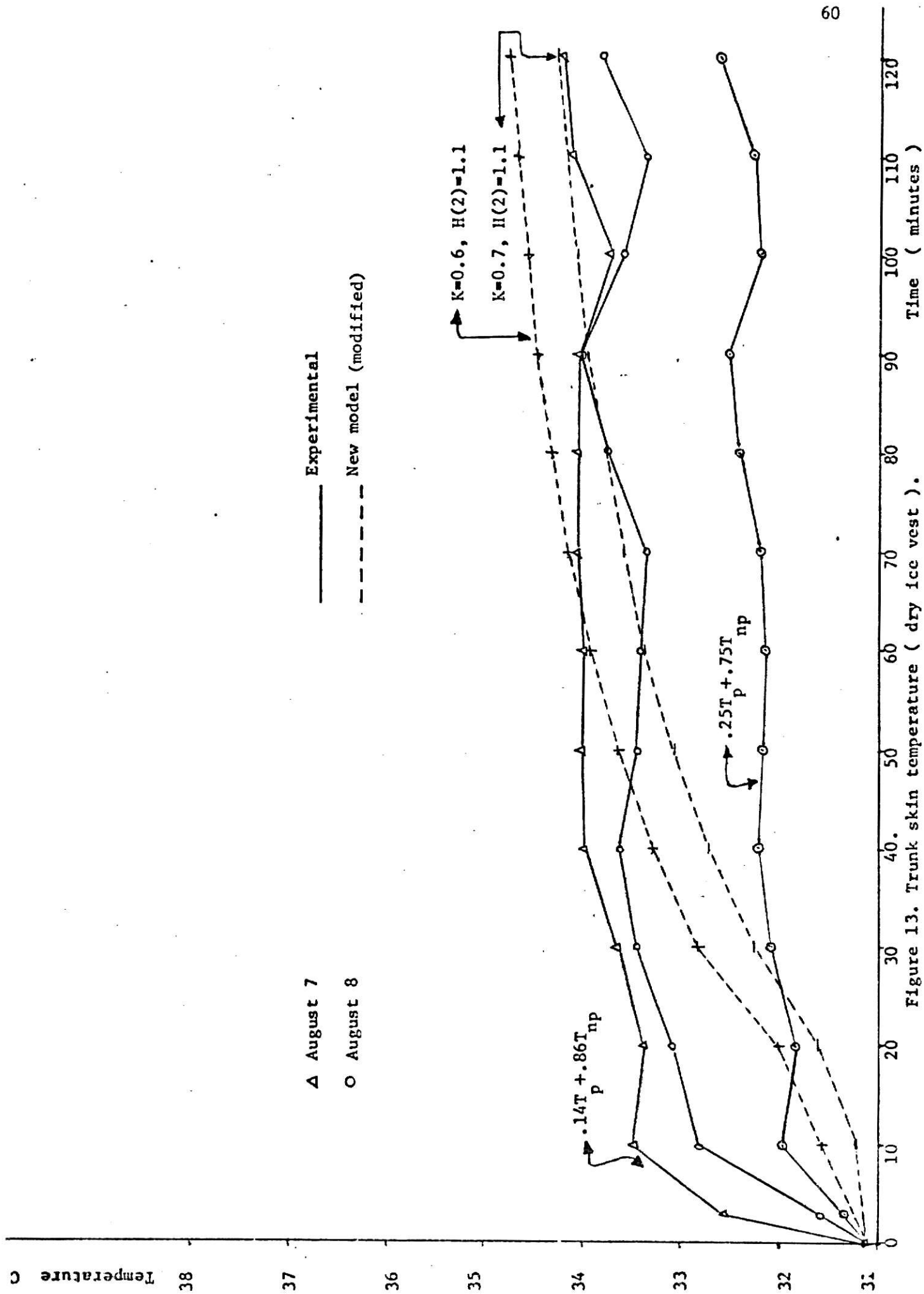


Figure 13. Trunk skin temperature (dry ice vest).

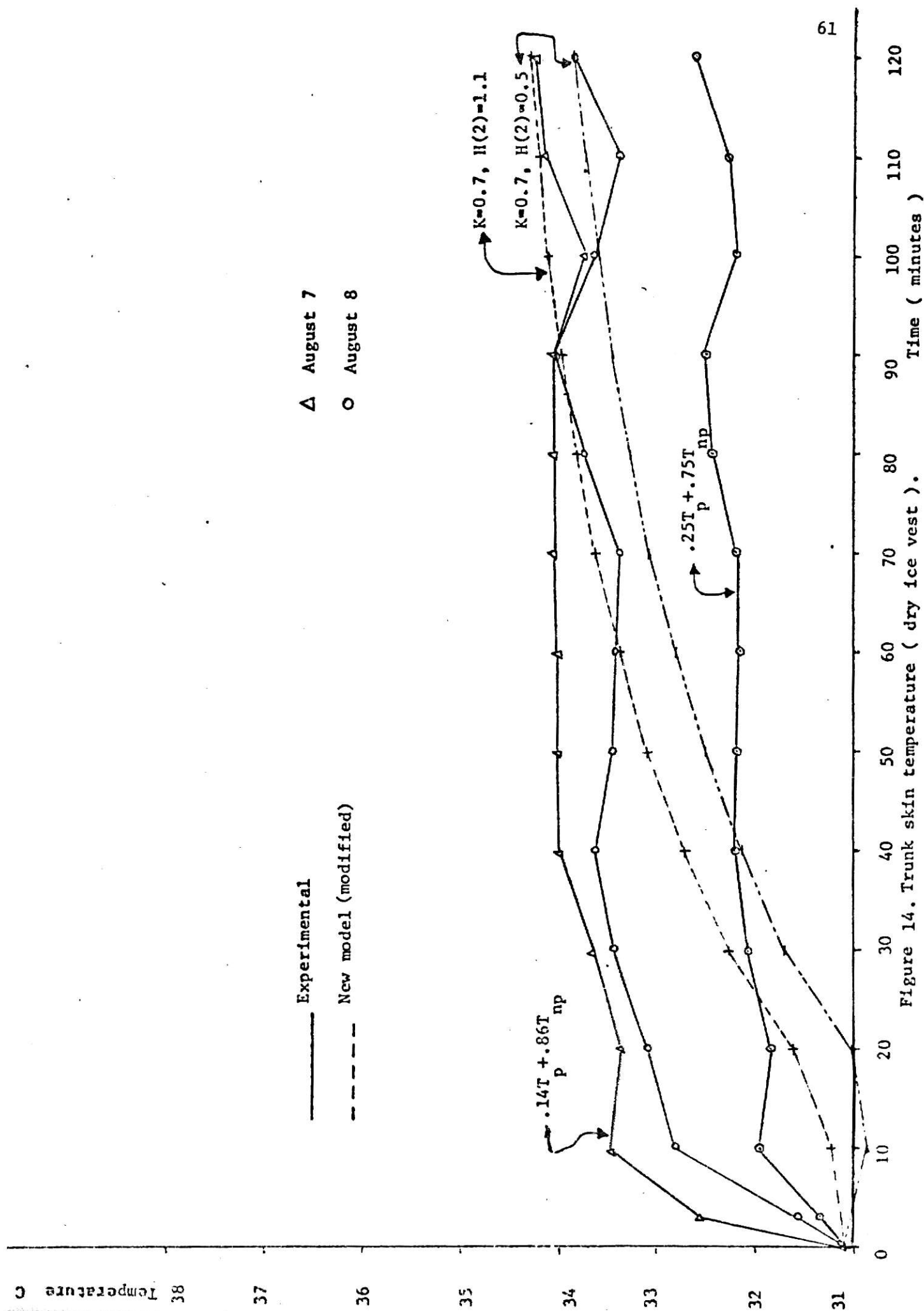


Figure 14. Trunk skin temperature (dry ice vest).

better fit is obtained for the trunk skin temperature by using the following values for the two parameters: $K=0.7$, $H(2)=1.1$. The simulated trunk skin temperature using the above values for K and $H(2)$ rose from 31.12 C at 0 min. to 34 C at 120 min. It is pointed out here that the estimated experimental trunk skin temperature is only an approximation and as such it is difficult to make an exact comparison between the simulated and the estimated trunk skin temperatures.

Figure 15 shows the arm skin temperature. The experimental values range from an average of 30.4 C at 0 minute to 37 C at 120 min. The model showed a rise in the arm skin temperature to about 35.9 C at 120 minutes. Thus the simulated result for the arm skin temperature is lower than the experimental value by 1.1 C.

Figure 16 shows the plot for the leg skin temperature. The simulated leg skin temperature rose from 31.05 at 0 min. to 36.5 C at 120 min. whereas the experimental temperatures for the two days lie on either side of the simulation line. Thus a good fit is indicated.

Figure 17 compares the cardiac output given by the model with $HR \times SBP$. The simulated cardiac output is in close agreement with $HR \times SBP$ ($HR \times SBP$ is used strictly as an index of experimental cardiac output and does not represent the true cardiac output of the subject).

Figure 18 shows the plots for the required sweat loss calculated from the heat balance equation from the experimental data (EVAPR) and the simulated value for evaporative heat loss given by the model (EV). EVAPR rose from 0 kcal/h at minute 0 to 108 at minute 120. In the model EV rose from 21 kcal/h at 0 minute to 80 at minute 120. The simulated value seems less than the estimated experimental value for EVAPR.

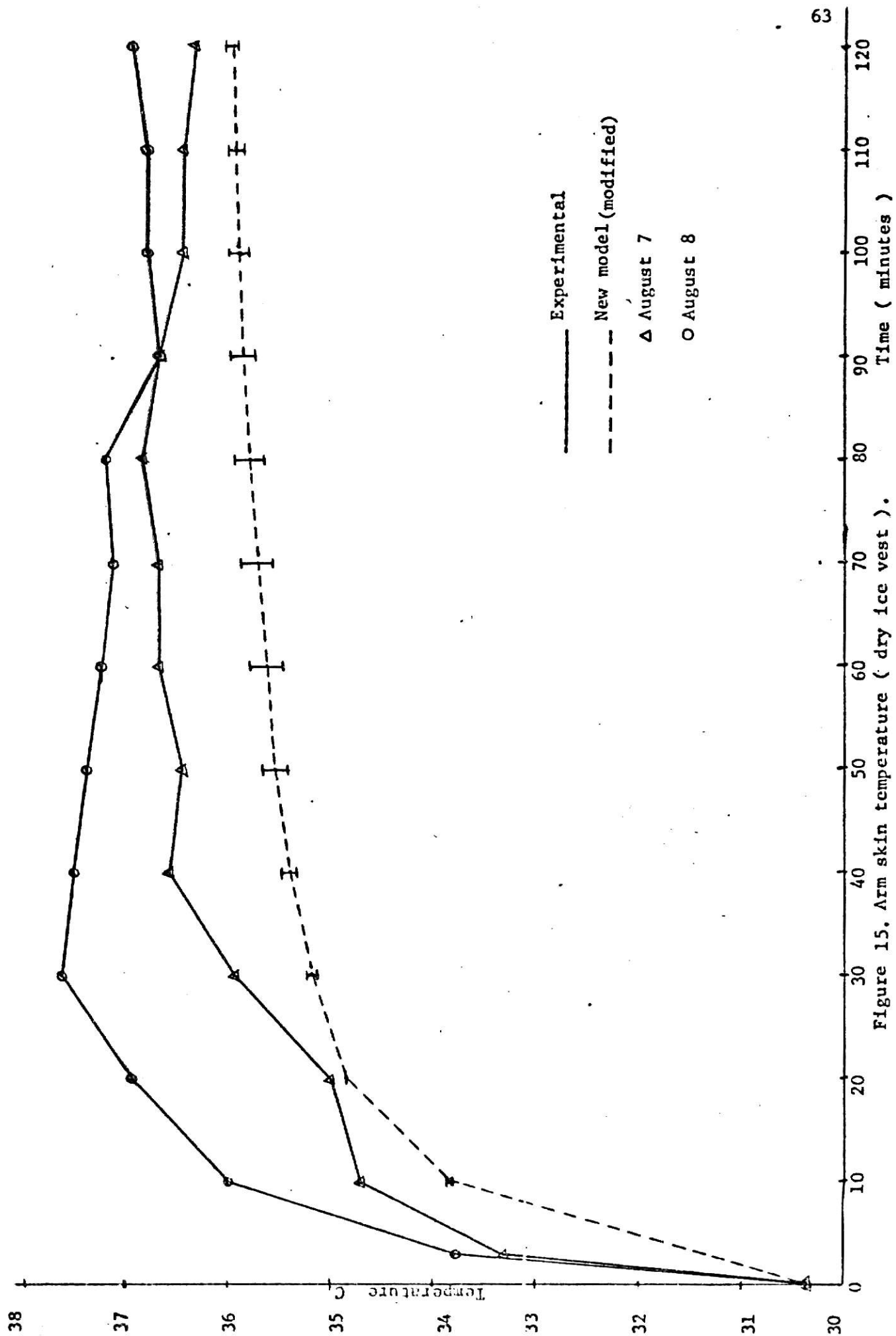


Figure 15. Arm skin temperature (dry ice vest).

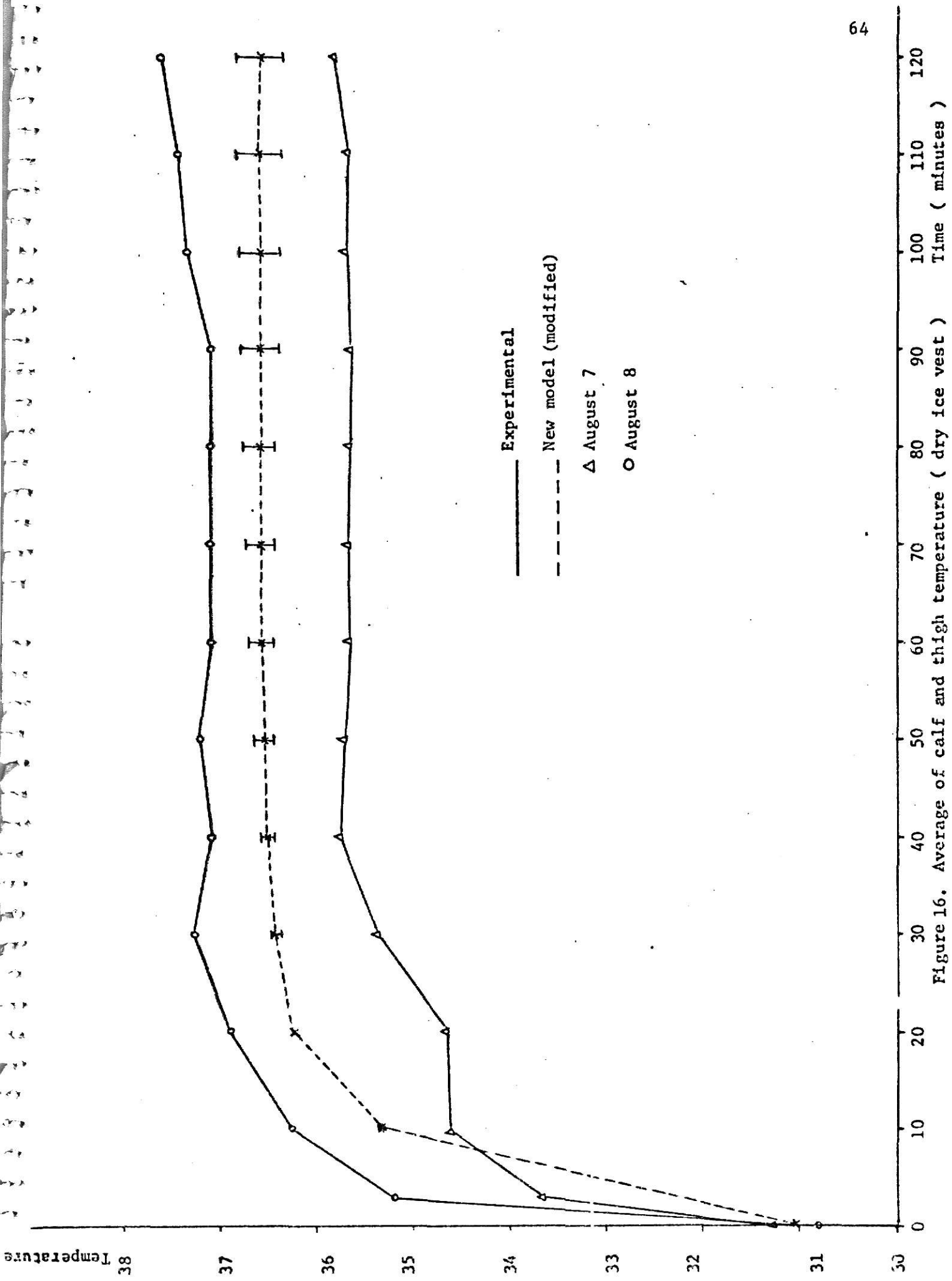


Figure 16. Average of calf and thigh temperature (dry ice vest)

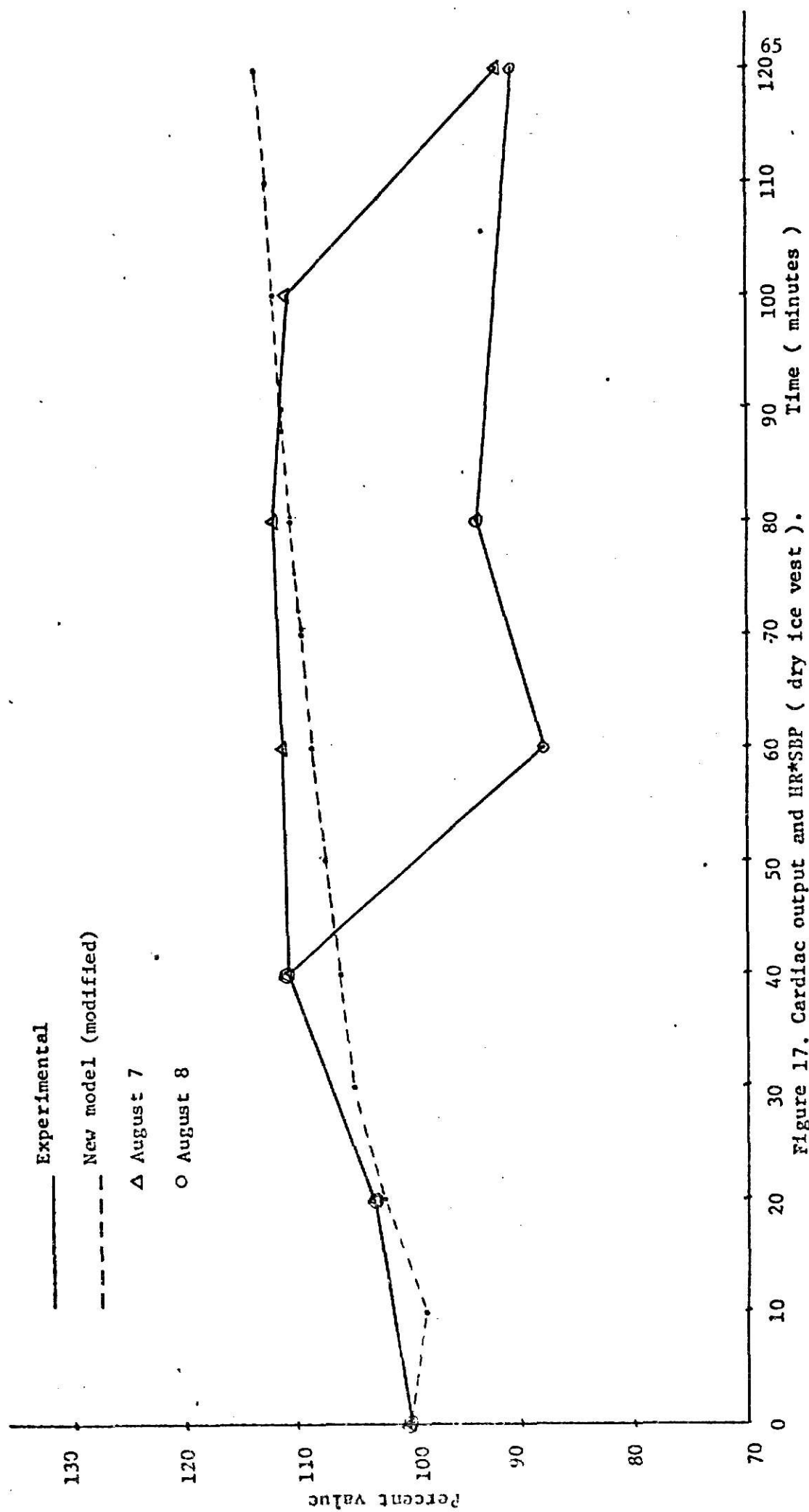


Figure 17. Cardiac output and HR*SDP (dry ice vest).

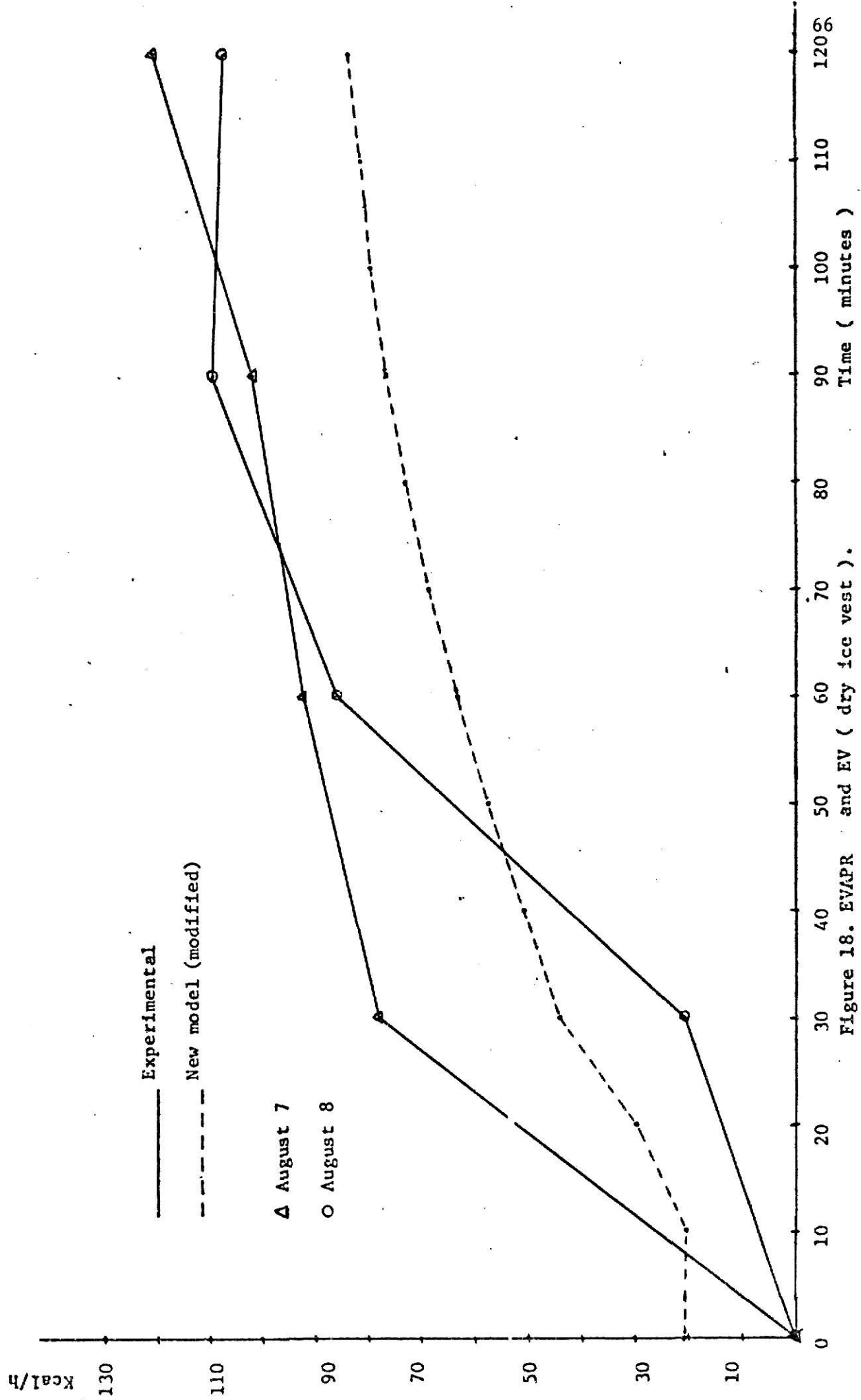


Figure 18. EV/APR and EV (dry ice vest).

DISCUSSION

This study used Stolwijk's models (1970, 1974). The new model, although having the same equations as the old model in most part, differed drastically from the old model in terms of the input data.

The function of the thermal regulatory mechanism is to balance the rates of heat production and heat loss at some body temperature that is near to the optimal temperature for some body functions. This optimal temperature is referred to as the set-point temperature. Table 13 shows the set-point temperatures for all the twenty-five body compartments.

Table 14 gives the initial input temperatures. The values of rectal, head skin, trunk skin, arm skin, and leg skin temperatures given in Table 14 represent experimental measurements taken on the subject. The remaining temperatures were derived using the values given by Stolwijk (38).

The experimental results indicate that personal cooling with dry ice can appreciably lower the thermal load on a person exposed to a heat stress environment. Comparing the experimental results for the nude man with those for the dry ice vest case we see that in the latter case:

- (1) Trunk skin temperature is lower (Figs. 6,13,14)
- (2) Index of cardiac output $HR \cdot SBP$ is lower (Figs. 9,17) thereby indicating reduced cardiac output.
- (3) EVAPR is smaller (Figs. 10,18). Thus there is reduced evaporative cooling due to the dry ice vest.

The simulation results indicate the same trend in respect of trunk skin temperature, cardiac output (CO), and evaporative sweat loss (EV). Thus two things are apparent:

TABLE 13

TSET(N), SET POINT TEMPERATURE FOR RECEPTORS IN N, DEG C

OLD MODEL

	CORE	MUSCLE	FAT	SKIN
HEAD	37.000	36.400	36.100	35.900
TRUNK	37.100	36.800	35.500	34.700
ARMS	35.600	35.000	34.500	34.300
HANDS	35.500	35.400	35.350	35.300
LEGS	36.400	35.800	35.000	34.700
FEET	35.500	35.300	35.400	35.300
CENTRAL BLOOD	36.94			

NEW MODEL

	CORE	MUSCLE	FAT	SKIN
HEAD	36.960	35.070	34.810	34.580
TRUNK	36.890	36.280	34.530	33.620
ARMS	35.530	34.120	33.590	33.250
HANDS	35.410	35.380	35.300	35.220
LEGS	35.810	35.300	35.310	34.100
FEET	35.140	35.030	35.110	35.040
CENTRAL BLOOD	36.71			

TABLE 14

INITIAL INPUT TEMPERATURES, DEG C

OLD MODEL

	CORE	MUSCLE	FAT	SKIN
HEAD	36.550	35.130	34.280	33.720
TRUNK	36.610	36.050	33.390	31.740
ARMS	35.100	33.500	31.960	31.330
HANDS	34.960	33.850	33.300	32.370
LEGS	35.950	34.440	32.590	31.950
FEET	34.950	32.330	34.030	32.490
CENTRAL BLOOD	36.46			

NEW MODEL

	CORE	MUSCLE	FAT	SKIN
HEAD	36.550	35.130	34.280	33.720
TRUNK	36.610	36.050	33.390	31.740
ARMS	35.100	33.500	31.960	31.330
HANDS	34.960	33.850	33.300	32.370
LEGS	35.950	34.440	32.590	31.950
FEET	34.950	32.330	34.030	32.490
CENTRAL BLOOD	36.46			

- (1) Dry ice cooling provides a useful microclimate for reducing thermal load on a person exposed to a heat stress environment.
- (2) The new model simulates the experimental results very well.

It should be possible to use the model to predict the length of time the human body can survive under a specific hostile environment. Mean body temperature, TB, is more important in any evaluation of thermal stress on the body than the surface skin temperature, TS. One formula estimates the mean body temperature as:

$$TB = 0.79 TR + .21 TS$$

where TR is the rectal temperature. From Figures 4 and 11 it is quite clear that the simulated trunk core temperature gives a close fit to the experimental rectal temperature. Even though the simulated skin temperatures are somewhat different than their experimental counterparts, the simulated mean body temperature should be quite close to the experimental mean body temperature because of the better prediction for the rectal temperature TR.

SUMMARY AND CONCLUSIONS

The model output is quite sensitive to changes in the values of the combined environmental heat transfer coefficients. $H(2)$, the combined environmental heat transfer coefficient for the trunk segment, was estimated to be $1.1 \text{ kcal.h}^{-1} \cdot ^\circ\text{C}^{-1}$. This in reality, may not be true. An extensive study of this important variable should, therefore, be included in future studies. In conclusion, it must be mentioned that the new Stolwijk model simulates the human thermal regulatory system very well as compared to the old model. The model should also help in designing suitable experiments for challenging expressed concepts of human thermoregulation because modeling and experimentation are part of a cycle in which experimental data form the basis of a conceptual proposal which in turn is challenged by suitably designed experiments. The useful life of a detailed quantitative model is no longer than one of these cycles.

REFERENCES

1. Aschoff, J., and Wever, R., "Kern und Schale im Warmehaushalt des Menschen", Naturwissenschaften, 45, 477-485, 1958.
2. Bader, M.E., and Macht, M.B., "Indirect peripheral vasodilation produced by the warming of various body areas", Journal Appl Physiol, 1:215-226, 1948.
3. Barbour, H.G., "Die Wirkung unmittelbarer Erwärmung und Abkühlung der Warmezentren auf die Körpertemperatur", Naunyn-Schmiedebergs Arch. exp. Path. Pharmac., 70, 1, 1912.
4. Bazett, H.C., and Penfield, W.G., "A study of the Sherrington decerebrate animal in the chronic as well as in the acute condition", Brain, 45, 185, 1922.
5. Benzinger, T.H., "The Human Thermostat", in Temperature-Its Measurement and Control in Science and Industry, Part III, Chapt. 56, p. 637. New York, Reinhold Publ. Corp. 1963.
6. Bligh, Temperature Regulation in Mammals and other Vertebrates, North Holland Publishing Company, 1973.
7. Bradfield, H.S., "The determination of surface area of women and its use in expressing basal metabolic rate", Amer J Physiol, 82:570-576, 1927.
8. Brebner, D.F., Kerslake, D. McK., and Waddell, J.L., "The relation between the coefficients for head exchange by convection and by evaporation in man", J Physiol, 141:164-168, 1958.
9. Brown, A.C., "Analog computer simulation of temperature regulation in man", Technical Documentary Report AMRL-TDR-63-116, Aerospace Medical Research Laboratories, Wright-Patterson AFB, Ohio, 1963.
10. Bullard, R.W., Bannerjee, M.R., and MacIntyre, B.A., "The role of the skin in negative feedback regulation of eccrine sweating", Int J Biometeor, 11:93-104, 1967.
11. Burton, A.C., "The application of the theory of heat flow to the study of energy metabolism", J Nutr., 7, 497, 1934.
12. Burton, D.R., and Collier, L., "The development of water conditioned suits", Technical Note No. Mech. Engr. 400, Royal Aircraft Est., April, 1964.
13. Cabanac, M., Stolwijk, J., and Hardy, J.D., "Effect of temperature and pyrogens on simple unit activity in the rabbit's brain stem", J Appl Physiol, 24:645-652, 1968.

14. Chambers, A.B., "Controlling thermal comfort in the EVA space suit", ASHRAE Journal, 12, 33-38, 1970.
15. Crosbie, R.J., Hardy, J.D., and Fessenden, E., "Electrical analgs of simulation of temperature regulation in man", in Temperature-Its Measurement and Control in Science and Industry, Part III, Chapt. 55, pp 627-635. New York, Reinhold Publ. Corp. 1963.
16. DuBois, D., and DuBois, E.F., "Clinical calorimetry: fifth paper, The measurement of surface area of man", Arch Internal Med, 15:868-888, 1915.
17. DuBois, D., and DuBois, E.F., "Clinical calorimetry: tenth paper, A formula to estimate the approximate surface area if height and weight be known", Arch Internal Med, 17:863-871, 1915.
18. Fan, L.T., Hsu, F.T., and Hwang, C.L., "A review on mathematical models of the human thermal system", IEEE Transactions on Biomed. Engg., BMI-18(3), May, 1971.
19. Hammel, H.T., Jackson, D.C., Stolwijk, J., Hardy, J.D., and Stromme, S.B., "Temperature regulation by hypothalamine proportional control with an adjustable set point", J Appl Physiol, 18:1146-1154, 1963.
20. Hardy, J. D., "Control of heat loss and heat production in physiologic temperature regulation", Harvey Lec. Ser. XLIX, 242, 1953-1954.
21. Hardy, J.D., and Hammel, H.T., "Control system in physiological temperature regulation", in Temperature-Its Measurement and Control in Science and Industry, Part III, Chapt. 54, p. 613. New York, Reinhold Publ. Corp. 1963.
22. Hemingway, A., "Effects of heating hypothalamus of dogs by diathermy", J Neurophysiol, 3,328, 1940.
23. Hertzman, A.B., and Randall, W.C., "Regional differences in the basal and maximal rates of blood flow in the skin", J Appl Physiol, 1:234-341, 1948.
24. Hsu, F.T., "Modeling, simulation, and optimal control of the human thermal system", Ph.D. Dissertation, Kansas State University, Manhattan, Kansas 1971.
25. Keller, A.D., and Hare, W.K., "The hypothalamus and heat regulation", Proc. Soc. exp. Biol. (N.Y.) 29, 1069, 1932.
26. Kerslake, D., The Stress of Hot Environments, Cambridge University Press, 1972.

27. Konz, S., Hwang, C., Perkins, R., and Borell, S., "Personal cooling with dry ice", American Industrial Hygiene Association Journal, 35, 3, March, 1974.
28. Layne, R. S., and Barker, R. S., "Digital computer simulation of the biothermal man", Paper No. 3369, Douglas Missile and Spacecraft Division, 1965.
29. Liebermeister, C., "Untersuchungen uber die quantitative Veranderung der Kohlensaureproduktion beim Menschen. Dtsch. Arch. klin. Med. 8, 153, 1971.
30. Magoun, H.W., Harrison, F., Brobeck, J.R., and Ranson, S.W., "Activation of heat loss mechanism by local heating of the brain", Journal of Neurophysiology, 1, 101-114, 1938.
31. Meeh, K., "Oberflächenmessungen des menschlichen", Korpers. Z Biol, 15:428-458, 1879.
32. Ott, T., "Heat center in the brain", J nerv. ment. Dis. 14, 152, 1887.
33. Perl, W., "Heat and matter distribution in body tissues and the determination of tissue blood flow by local clearance methods", J Theoretical Biology, 2, 201-235, 1962.
34. Randall, W.C., "Quantitation and regional distribution of sweat glands in man", J Clin Invest, 25:761-767, 1946.
35. Richet, C., "Die Beziehung des Gehirns zur Körperwärme und zum Fieber", Pflugers Arch. ges. Physiol. 37, 624, 1885.
36. Scammon, R. E., "Developmental anatomy", in Schaeffer, J.P. (Ed.), Morris' Human Anatomy, 11th ed. New York, McGraw-Hill, 1953.
37. Smith, P.E., and James, E.W. II, "Human responses to heat stress", Arch Environ Health, 9:323-342, 1964.
38. Stolwijk, J., "Mathematical models of thermoregulation", in Physiological and Behavioral Temperature Regulation, Chapt. 48, p. 703. Springfield, Ill., Charles C. Thomas, 1970.
39. Stolwijk, J., Private Communication to Dr. C.L. Hwang, July, 1974.
40. Stolwijk, J., and Cunningham, D.J., "A study of heat exchange between man and his environment in Project Apollo", Contract No. NAS-9-4522, Final Report, John B. Pierce Foundation.
41. Stolwijk, J., and Hardy, J.D., "Partitional calorimetric studies of responses of man to thermal transients", J Appl Physiol, 21:967-977, 1966.

42. Stolwijk, J., and Hardy, J.D., "Temperature regulation in man - A theoretical study", Pflugers Arch Ges Physiol, 291:129-162, 1966.
43. Stolwijk, J., Saltin, B., and Gagge, A.P., "Physiological factors associated with sweating during exercise", J Aerospace Med, 39:1101-1105, 1968.
44. Thauer, R., "Der nervose Mechanismus der chemischen Temperaturregulation des Warmbluters", Naturwissenschaften 51, 73 (1964).
45. van Graan, C.H., "The determination of body surface area", S.A. Medical Journal, 43, 952-959, Aug. 1969.
46. Wilmer, H.A., "Changes in structural components of human body from six lunar months to maturity", Proc Soc Exp Biol Med, 43:545-547, 1940.
47. Wissler, E.H., "Steady state temperature distribution in man", Journal of Appl Physiol, 16, 1961.
48. Wissler, E.H., "An analysis of factors affecting temperature levels in the nude human", in J.D. Hardy (Ed.), Temperature-Its Measurement and Control in Science and Industry, Part III, Chapt. 53. New York, Reinhold Publ. Corp., 1963.
49. Wissler, E.H., "A mathematical model of the human thermal system", Bulletin of Mathematical Biophysics, 26, 147-166, 1964.
50. Wissler, E.H., "Comparison of computer results from two mathematical models - A simple 14- node model and a complex 250-node model", Symposium International de Thermoregulation Comportementale, Lyon, France, 7-11 Sept., 1970.
51. Wyndham, C.H., and Atkins, A.R., "Approach to solution of human biothermal problem with the aid of an analog computer", Paper No. 27 3rd Int. Conference on Medical Electronics, 1960.
52. Yamamoto, W.S., and Raub, W.F., "Models of the regulation of internal respiration in mammals. Problems and promises", Computers and Biomed Res, 1:65-104, 1967.

APPENDIX

The appendix gives a complete listing of the FORTRAN program for implementing the revised human thermoregulatory model with dry ice cooling.

MAIN

```

    DIMENSION C(25),T(25),F(25),HF(25),TC(24),TD(24),QB(24),Q(24),
    1EB(24),E(24),BFB(24),BF(24),BC(24),HC(6),S(6),HR(6),H(6),P(10),
    2EMAX(6),TSET(25),ERROR(25),RATE(25),COLD(25),WARM(25),SKINR(6),
    3SKINS(6),SKINV(6),SKINC(6),WORKM(6),CHILM(6),TI(25),PSKIN(6),
    4SWPCP(6),TAIR(6),PAIR(6)
    REAL LTIME,ITIME

```

C READ CONSTANTS FOR CONTROLLED SYSTEM

```

100 FORMAT(14F5.2)
200 FORMAT(I2)
959 FORMAT(1H0,19X,'CORE',9X,'MUSCLE',9X,'FAT',9X,'SKIN'/5X,'HEAD ',4(
    15X,F9.3)/5X,'TRUNK ',4(5X,F9.3)/5X,'ARMS ',4(5X,F9.3)/5X,'HANDS ',4(
    25X,F9.3)/5X,'LEGS ',4(5X,F9.3)/5X,'FEET ',4(5X,F9.3))
960 FORMAT(1H0,19X,'CORE',9X,'MUSCLE',9X,'FAT',9X,'SKIN'/5X,'HEAD ',4(
    15X,F9.3)/5X,'TRUNK ',4(5X,F9.3)/5X,'ARMS ',4(5X,F9.3)/5X,'HANDS ',4(
    25X,F9.3)/5X,'LEGS ',4(5X,F9.3)/5X,'FEET ',4(5X,F9.3)/5X,'CENTRAL B
    3LOOD',F6.2)
961 FORMAT(1H0,15X,'HEAD ',5X,'TRUNK ',3X,'ARMS ',5X,'HANDS ',4X,'LEGS ',6
    1X,'FEET ',2X,'UNITS ')
962 FORMAT(1H0,4X,'PSKIN ',6(1X,F8.3),' MM HG ')
963 FORMAT(1H0,4X,'EMAX ',6(1X,F8.3),' KCAL/HR ')
964 FORMAT(1H0,4X,'SWPCP ',6(1X,F8.3))
965 FORMAT(1H0,4X,'H(I) ',6(1X,F8.3),' KCAL/HR/DEG C ')
966 FORMAT(1H0,4X,'S(I) ',6(1X,F8.4),' SQ. M ')
967 FORMAT(1H0,4X,'HR(I) ',6(1X,F8.3),' KCAL/SQ. M/HR/DEG C ')
968 FORMAT(1H0,4X,'HC(I) ',6(1X,F8.3),' KCAL/SQ. M/HR/DEG C ')
970 FORMAT(1H0,4X,'SKINR(I)',6(1X,F8.3))
971 FORMAT(1H0,4X,'SKINS(I)',6(1X,F8.3))
972 FORMAT(1H0,4X,'SKINV(I)',6(1X,F8.3))
973 FORMAT(1H0,4X,'SKINC(I)',6(1X,F8.3))
974 FORMAT(1H0,4X,'WORKM(I)',6(1X,F8.3))
975 FORMAT(1H0,4X,'CHILM(I)',6(1X,F8.3))
976 FORMAT(1H0,4X,'TAIR(I) ',6(1X,F8.2),' DEG C ')
101 CONTINUE
    READ(5,100)(C(I),I=1,25)
    READ(5,100)(QB(I),I=1,24)
    READ(5,100)(EB(I),I=1,24)
    READ(5,100)(BFB(I),I=1,24)
    READ(5,100)(TC(I),I=1,24)
    READ(5,100)(S(I),I=1,6)
    READ(5,100)(HR(I),I=1,6)
    READ(5,100)(HC(I),I=1,6)
    READ(5,100)(P(I),I=1,10)

```

C READ CONSTANTS FOR THE CONTRCLLER

```

    READ(5,100)(TSET(I),I=1,25)
    READ(5,100)(RATE(I),I=1,25)
    READ(5,100)CSW,SSW,PSW,COIL,SDIL,PDIL,CCON,SCON,PCON,CCHIL,SCHIL,
    XPCHIL
    READ(5,100)(SKINR(I),I=1,6)
    READ(5,100)(SKINS(I),I=1,6)
    READ(5,100)(SKINV(I),I=1,6)
    READ(5,100)(SKINC(I),I=1,6)
    READ(5,100)(WORKM(I),I=1,6)
    READ(5,100)(CHILM(I),I=1,6)

```

C READ INITIAL CONDITIONS

```

    READ(5,100)(T(I),I=1,25)
    WRITE(6,911)
911 FORMAT(1H0,4X,'CONSTANT DATA *****')
    WRITE(6,980)

```



```

980 FORMAT(1H0,4X,'C(I),      KCAL/DEG C ')
    WRITE(6,960)(C(I),I=1,25)
    WRITE(6,981)
981 FORMAT(1H0,4X,'QB(I),      KCAL/HR  ')
    WRITE(6,959)(QB(I),I=1,24)
    WRITE(6,982)
982 FORMAT(1H0,4X,'EB(I),      KCAL/HR  ')
    WRITE(6,959)(EB(I),I=1,24)
    WRITE(6,983)
983 FORMAT(1H0,4X,'BFB(I),     LITRES/HR ')
    WRITE(6,959)(BFB(I),I=1,24)
    WRITE(6,984)
984 FORMAT(1H0,4X,'TC(I),      KCAL/HR/DEG C ')
    WRITE(6,959)(TC(I),I=1,24)
    WRITE(6,985)
985 FORMAT(1H0,4X,'TSET(I),     DEG C  ')
    WRITE(6,960)(TSET(I),I=1,25)
    WRITE(6,986)
986 FORMAT(1H0,4X,'RATE(I)')
    WRITE(6,960)(RATE(I),I=1,25)
    WRITE(6,961)
    WRITE(6,966)(S(I),I=1,6)
    WRITE(6,967)(HR(I),I=1,6)
    WRITE(6,968)(HC(I),I=1,6)
    WRITE(6,970)(SKINR(I),I=1,6)
    WRITE(6,971)(SKINS(I),I=1,6)
    WRITE(6,972)(SKINV(I),I=1,6)
    WRITE(6,973)(SKINC(I),I=1,6)
    WRITE(6,974)(WORKM(I),I=1,6)
    WRITE(6,975)(CHILM(I),I=1,6)
    WRITE(6,890)
890 FORMAT(1H0,4X,'INITIAL INPUT TEMPERATURES, DEG C')
    WRITE(6,960)(T(I),I=1,25)
    TIME=0.
    ITIME=0.
    DO 102 N=1,25
    F(N)=0
102 CONTINUE
C      READ EXPERIMENTAL CONDITIONS
103 CONTINUE
    READ(5,100)(TAIR(I),I=1,6)
    WRITE(6,976)(TAIR(I),I=1,6)
    READ(5,100)V
    WRITE(6,894)V
894 FORMAT(1H0,4X,'AIR VELOCITY=',F8.2,' M/SEC')
    READ(5,100)RH
    WRITE(6,896)RH
896 FORMAT(1H0,4X,'RELATIVE HUMIDITY=',F8.2)
    READ(5,100)WORK
    IF(WORK-86.5)104,104,105
104 WORK=0.
    GO TO 106
105 WORK=(WORK-86.5)*0.78
106 CONTINUE
    READ(5,200)INT
    WRITE(6,898)INT
898 FORMAT(1H0,4X,'OUTPUT INTERVAL=',I2,' MINUTES')
    WRITE(6,893)

```

```

893 FORMAT(1H0,4X,'TIME=0.0 *****')
DO 202 J=1,6
H(J)=(HR(J)+3.16*HC(J)*V**0.5)*S(J)
I=TAIR(J)/5
PAIR(J)=RH*(P(I)+(P(I+1)-P(I))*(TAIR(J)-5*I)/5.)
202 CONTINUE
C      ESTABLISH THERMORECEPTOR OUTPUT
301 CONTINUE
DO 302 N=1,25
WARM(N)=0.
COLD(N)=0.
ERROR(N)=T(N)-TSET(N)+RATE(N)*F(N)
IF(ERROR(N))303,302,304
303 COLD(N)=-ERROR(N)
GO TO 302
304 WARM(N)=ERROR(N)
302 CONTINUE
C      INTEGRATE PERIPHERAL AFFERENTS
WARMS=0.0
COLDS=0.0
DO 305 I=1,6
K=4*I
WARMS=WARMS+WARM(K)*SKINR(I)
COLDS=COLDS+COLD(K)*SKINR(I)
305 CONTINUE
C      DETERMINE EFFERENT OUTFLOW
SWEAT=CSW*ERROR(1)+SSW*(WARMS-COLDS)+PSW*ERROR(1)*(WARMS-COLDS)
DILAT=CDIL*ERROR(1)+SDIL*(WARMS-COLDS)+PDIL*WARM(1)*WARMS
STRIC=-CCON*ERROR(1)-SCON*(WARMS-COLDS)+PCON*COLD(1)*COLDS
CHILL=(CCHIL*ERROR(1)+SCHIL*(WARMS-COLDS))*PCHIL*(WARMS-COLDS)
IF(SWEAT)1500,1500,1501
1500 SWEAT=0.0
1501 CONTINUE
IF(DILAT)1502,1502,1503
1502 DILAT=0.0
1503 CONTINUE
IF(STRIC)1504,1504,1505
1504 STRIC=0.0
1505 CONTINUE
IF(CHILL)1506,1506,1507
1506 CHILL=0.0
1507 CONTINUE
C      ASSIGN EFFECTOR OUTPUT
400 CONTINUE
DO 401 I=1,6
SWPCP(I)=SKINS(I)*SWEAT
N=4*I-3
BF(N)=BFB(N)
Q(N)=QB(N)
E(N)=EB(N)
Q(N+1)=QB(N+1)+WORKM(I)*WORK+CHILM(I)*CHILL
E(N+1)=0
BF(N+1)=BFB(N+1)+Q(N+1)-QB(N+1)
Q(N+2)=QB(N+2)
E(N+2)=0
BF(N+2)=BFB(N+2)
Q(N+3)=QB(N+3)
E(N+3)=EB(N+3)+SKINS(I)*SWEAT*2.**((T(N+3)-TSET(N+3))/4.)

```

```

BF(N+3)=(BFB(N+3)+SKINV(I)*DILAT)/(L+SKINC(I)*STRIC)
K=T(N+3)/5.
PSKIN(I)=P(K)+(P(K+1)-P(K))*(T(N+3)-5*K)/5.
EMAX(I)=(PSKIN(I)-PAIR(I))*2.14*(H(I)-HR(I)*S(I))
IF(EMAX(I)-E(N+3))402,403,403
402 E(N+3)=EMAX(I)
403 CONTINUE
401 CONTINUE
C          CALCULATE HEAT FLOWS
DO 500 K=1,24
BC(K)=BF(K)*(T(K)-T(25))
TD(K)=TC(K)*(T(K)-T(K+1))
500 CONTINUE
DO 501 I=1,6
K=4*I-3
HF(K)=Q(K)-E(K)-BC(K)-TD(K)
HF(K+1)=Q(K+1)-BC(K+1)+TD(K)-TD(K+1)
HF(K+2)=Q(K+2)-BC(K+2)+TD(K+1)-TD(K+2)
HF(K+3)=Q(K+3)-BC(K+3)-E(K+3)+TD(K+2)-H(I)*(T(K+3)-TAIR(I))
501 CONTINUE
HF(8)=HF(8)-(0.517*137.*.75)
HF(25)=0.0
DO 502 K=1,24
HF(25)=HF(25)+BC(K)
502 CONTINUE
HF(25)=HF(25)-0.08*WORK
C          DETERMINE OPTIMUM INTEGRATION STEP
DT=0.016666667
DO 600 K=1,25
F(K)=HF(K)/C(K)
U=ABS(F(K))
IF(U*DT-0.1)600,600,601
601 DT=0.1/U
600 CONTINUE
C          CALCULATE NEW TEMPERATURES
DO 700 K=1,25
T(K)=T(K)+F(K)*DT
700 CONTINUE
TIME=TIME+DT
LTIME=60.*TIME
IF(LTIME-INT-LTIME)301,701,701
701 CONTINUE
WRITE(6,910)SWEAT
910 FORMAT(1H0,/////////'      SWEAT= ',F9.3)
WRITE(6,961)
WRITE(6,962)(PSKIN(I),I=1,6)
WRITE(6,963)(EMAX(I),I=1,6)
WRITE(6,964)(SWPCP(I),I=1,6)
WRITE(6,965)(H(I),I=1,6)
WRITE(6,931)
931 FORMAT(1H0,4X,'TEMPERATURES, DEG C')
WRITE(6,960)(T(K),K=1,25)
WRITE(6,900)
900 FORMAT(1H0,4X,'METABOLIC HEAT PRODUCTION,      KCAL/HR ')
WRITE(6,959)(Q(N),N=1,24)
WRITE(6,901)
901 FORMAT(1H0,4X,'BLOOD FLOWS,LITRES/HR')
WRITE(6,959)(BF(I),I=1,24)

```

```

WRITE(6,906)
906 FORMAT(1H0,4X,'EVAPORATIVE HEAT LOSS,      KCAL/HR ')
WRITE(6,959)(E(N),N=1,24)
WRITE(6,902)
902 FORMAT(1H0,4X,'BC,      KCAL/HR')
WRITE(6,959)(BC(K),K=1,24)
WRITE(6,903)
903 FORMAT(1H0,4X,'TD,      KCAL/HR ')
WRITE(6,959)(TD(K),K=1,24)
WRITE(6,904)
904 FORMAT(1H0,4X,'HEAT FLOWS,      KCAL/HR ')
WRITE(6,960)(HF(K),K=1,25)
WRITE(6,905)
905 FORMAT(1H0,4X,'RATE OF CHANGE OF TEMPERATURE, DEG C/HR')
WRITE(6,960)(F(K),K=1,25)
WRITE(6,940)LTIME
940 FORMAT(1H0,4X,'LTIME=',F8.3,' MINUTES')
C      PREPARE FOR OUTPUT
CO=0.
HP=0.
EV=0.
TS=0.
TB=0.
HFLOW=0.
SBF=0.
DO 800 N=1,24
CO=CO+BF(N)/60.
HP=HP+Q(N)
EV=EV+E(N)
800 CONTINUE
EV=EV+0.08*WORK
WRITE(6,950)CO
950 FORMAT(1H0,4X,'CO=',F9.3,' LITRES/MINUTE')
WRITE(6,951)HP
951 FORMAT(1H0,4X,'HP=',F9.3)
WRITE(6,952)EV
952 FORMAT(1H0,4X,'EV=',F9.3)
DO 802 I=1,6
SBF=SBF+BF(4*I)/60.
TS=TS+T(4*I)*C(4*I)/3.90
802 CONTINUE
WRITE(6,953)TS
953 FORMAT(1H0,4X,'TS=',F9.3,' DEG C')
WRITE(6,907)SBF
907 FORMAT(1H0,4X,'SKIN BLOOD FLOWS = ',F9.3,' LITRES/MT ')
ITIME=ITIME+INT
WRITE(6,941)ITIME
941 FORMAT(1H0,4X,'ITIME=',F8.0,' MINUTES')
DO 801 N=1,25
TB=TB+T(N)*C(N)/68.79
HFLOW=HFLOW+HF(N)
801 CONTINUE
WRITE(6,954)TB
954 FORMAT(1H0,4X,'TB=',F9.3,' DEG C')
IF(ITIME-120)301,803,803
803 CONTINUE
STOP
END

```

SIMULATION OF A HUMAN THERMOREGULATORY SYSTEM
WITH DRY ICE COOLING

by

BALDEV SINGH DHIMAN

B.S. (Engg), Punjab University, 1969

AN ABSTRACT OF A MASTER'S THESIS

submitted in partial fulfilment of the
requirements for the degree

MASTER OF SCIENCE

in

INDUSTRIAL ENGINEERING

Department of Industrial Engineering

KANSAS STATE UNIVERSITY

Manhattan, Kansas

1974

ABSTRACT

Dry ice cooling can provide a useful micro-climate for the purpose of personal cooling. Before its use in practical situations, it is desirable to evaluate experimental data. An analytic model based upon Stolwijk's models (1970 and 1974) was developed to simulate the process of thermoregulatory cooling of the human body when provided with an external cooling device (a dry ice vest). The model simulated the response of the human thermal regulatory system exposed to a heat stress environment (43.3 C and RH of 50%) for two types of situations:

(1) nude man (2) man wearing a dry ice vest.

We compared the simulated response (given by the model) vs the data gathered by Konz et al in 1972. This comparison was made for rectal, head skin, trunk skin, arm skin, and leg skin temperature, cardiac output, and evaporative sweat loss. The new Stolwijk model gave consistently better results in all the above comparisons than the old model although in the case of the nude man, both models gave a fairly close fit to the experimental rectal temperature. For the new model, simulated head skin temperature at 120 min. was more than experimental by 0.5 C, trunk skin was less by 0.5 C, arm skin was less by 0.8 C, and leg skin was less by 1.0 C. For cardiac output, simulated was lower than experimental by 15%. For evaporation simulated was higher by 4 kcal/h.

For the case of the man wearing a dry ice vest, only the new model was employed for simulations. The differences between simulation and experiment at 120 min. were as follows: rectal temperature -0.2 C, head skin +0.2 C, trunk skin +0.5 C, arm skin -0.8 C, leg skin 0.0 C, cardiac output + 10%, and evaporative sweat loss -28 kcal/h.